Chinese Journal of Natural Medicines

Dammarane-type triterpenoids from *Gynostemma longipes* and their protective activities on hypoxia-induced injury in PC12 cells

Haizhen LIANG, Xiaojuan CHEN, Qi LI, Mengmeng ZHANG, Pengxin LU, Jie ZHANG, Juan SONG, Tao ZHANG, Baolin GUO, Baiping MA

Citation: Haizhen LIANG, Xiaojuan CHEN, Qi LI, Mengmeng ZHANG, Pengxin LU, Jie ZHANG, Juan SONG, Tao ZHANG, Baolin GUO, Baiping MA, Dammarane-type triterpenoids from *Gynostemma longipes* and their protective activities on hypoxia-induced injury in PC12 cells, Chinese Journal of Natural Medicines, 2024, 22(5), 466-480. doi: 10.1016/S1875-5364(24)60643-6.

View online: https://doi.org/10.1016/S1875-5364(24)60643-6

Available online at www.sciencedirect.com
ScienceDirect
Chinese Journal of Natural Medicines 2024, **22**(5): 466-480
doi: 10.1016/S1875-5364(24)60643-6
Chinese Journal of Natural Medicines

•Original article•

Dammarane-type triterpenoids from *Gynostemma longipes* and their protective activities on hypoxia-induced injury in PC12 cells

LIANG Haizhen[1Δ], CHEN Xiaojuan[1Δ], LI Qi[1], ZHANG Mengmeng[1], LU Pengxin[1], ZHANG Jie[1], SONG Juan[1], ZHANG Tao[3], GUO Baolin[2], MA Baiping[1*]

[1] *Department of Pharmaceutical Sciences, Beijing Institute of Radiation Medicine, Beijing 100850, China;*
[2] *Institute of Medicinal Plant Development, Chinese Academy of Medical Sciences & Peking Union Medical College, Beijing 100193, China;*
[3] *AnKang Chia Tai Pharmaceutical Co., Ltd., Shaanxi 725000, China*

Available online 20 May, 2024

[ABSTRACT] Sixteen new dammarane-type triterpenoid saponins (**1–16**) featuring diverse structural variations in the side chain at C-17, along with twenty-one known analogues (**17–37**), have been isolated from the rhizomes of *Gynostemma longipes* C. Y. Wu, a plant renowned for its medicinal and edible properties. The structural elucidation of these compounds was accomplished through comprehensive analyses of 1D and 2D NMR and HRMS spectroscopic data, supplemented by comparison with previously reported data. Subsequent assays on the isolates for their protective effects against hypoxia-induced damage in pheochromocytoma cells (PC12 cells) revealed that nine saponins exhibited significant anti-hypoxic activities. Further investigation into the anti-hypoxia mechanisms of the representative saponins demonstrated that compounds **22** and **36** markedly reduced the levels of hypoxia-induced apoptosis. Additionally, these compounds were found to decrease the release of lactate dehydrogenase (LDH) and malondialdehyde (MDA), while increasing the activity of superoxide dismutase (SOD), thereby indicating that the saponins could mitigate hypoxia-induced injuries by ameliorating apoptosis and oxidative stress. These findings offer substantial evidence for the future utilization and development of *G. longipes*, identifying dammarane-type triterpenoid saponins as its active anti-hypoxic constituents.

[KEY WORDS] *Gynostemma longipes*; Dammarane-type saponins; Anti-hypoxia effect; Apoptosis
[CLC Number] R965, R284 **[Document code]** A **[Article ID]** 2095-6975(2024)05-0466-15

Introduction

Gynostemma longipes C. Y. Wu, belonging to the genus *Gynostemma* within the Cucurbitaceae family, is predominantly found throughout the southern regions of China, extending from the Qinling Mountains to the Yangtze River. Recognized as one of the source plants for the traditional Chinese medicine Herba Gynostemma, or "*Jiaogulan*" in Chinese, it serves dual purposes, both medicinal and edible, and has been utilized in various capacities, including pharmaceutical raw materials and food ingredients, for managing conditions such as hypertension, diabetes, obesity, and hepatosteatosis [1, 2]. Phytochemical studies have identified dammarane-type triterpenoid saponins, known as gypenosides, as the primary bioactive constituents in *Gynostemma* species, exhibiting anti-hyperlipidemic, anti-cancer, and cardioprotective effects, among others [3-5]. To date, over 300 gypenosides have been isolated and characterized from *Gynostemma* species [6]. Despite this, only a limited number of studies have been published on the triterpenoid components of *G. longipes*, with a total of 33 triterpene isolates reported [7-9].

The anti-hypoxia activity of gypenosides from *Gynostemma* has garnered significant interest recently [10]. Hypoxia, which can be induced by various factors such as high altitude, impacts physiological functions and metabolic states, potentially leading to numerous diseases. It is a primary cause of death when affecting the brain, heart, and other critical organs. Research has demonstrated that dammarane-type saponins from *G. pentaphyllum* can effectively mitigate hypoxia-induced injuries [11].

In pursuit of further bioactive natural products that contribute to anti-hypoxia activity in *G. longipes*, a systematic investigation of the rhizomes' extract has yielded sixteen new gypenosides (**1–16**) with structurally diverse side chains at C-17, along with twenty-one known analogues (**17–37**). These

[Received on] 12-Oct.-2023
[*Corresponding author] E-mail: mabaiping@sina.com
[Δ]These authors contributed equally to this work.
These authors have no conflict of interest to declare.

isolated saponins can be categorized into two types based on the side chain at C-17 of the aglycone. Compounds **1**−**13** and **18**−**30**, belonging to type I, feature a side chain at C-17 that is cyclized into a diverse five-membered ring, while compounds **15**−**16** and **31**−**37**, classified as type II, have a typical linear chain as their side chain at C-17. All isolated compounds were assessed for their protective effects against hypoxia-induced injury in pheochromocytoma cells (PC12 cells), with representative compounds selected for further examination of their potential anti-hypoxia mechanisms (Fig. 1).

Results and Discussion

Compound **1** was isolated as white amorphous powder. Its molecular formula was established as $C_{52}H_{86}O_{22}$ based on HR-ESI-MS at *m/z* 1061.5546 $[M - H]^-$ (Calcd. for $C_{52}H_{85}O_{22}$, 1061.5532). The ^{1}H NMR spectrum of **1** revealed characteristic signals for six aglycone methyl groups (δ_H 0.91, 0.92, 1.11, 1.25, 1.27 and 1.47) and four anomeric protons [δ_H 4.84 (1H, d, J = 7.8 Hz), 4.91 (1H, d, J = 5.6 Hz), 5.03 (1H, d, J = 7.4 Hz) and 6.17 (1H, brs)]. A 3β -OH substitution was indicated by the chemical shift at δ_H 3.34 (1H, dd, J = 4.0, 12.1 Hz)[12]. The ^{13}C NMR data provided 52 signals, identifying 30 carbons belonging to the aglycone and 22 to sugar moieties. The 1D NMR spectroscopic data of the aglycone moiety of compound **1** were similar to those of gynoside C [13] with the exception of an additional aldehyde group at C-19 [δ_H 10.35 (1H, s); δ_C 205.7] and the absence of a hydroxy group at C-12 (δ_C 26.0), suggesting compound **1** to

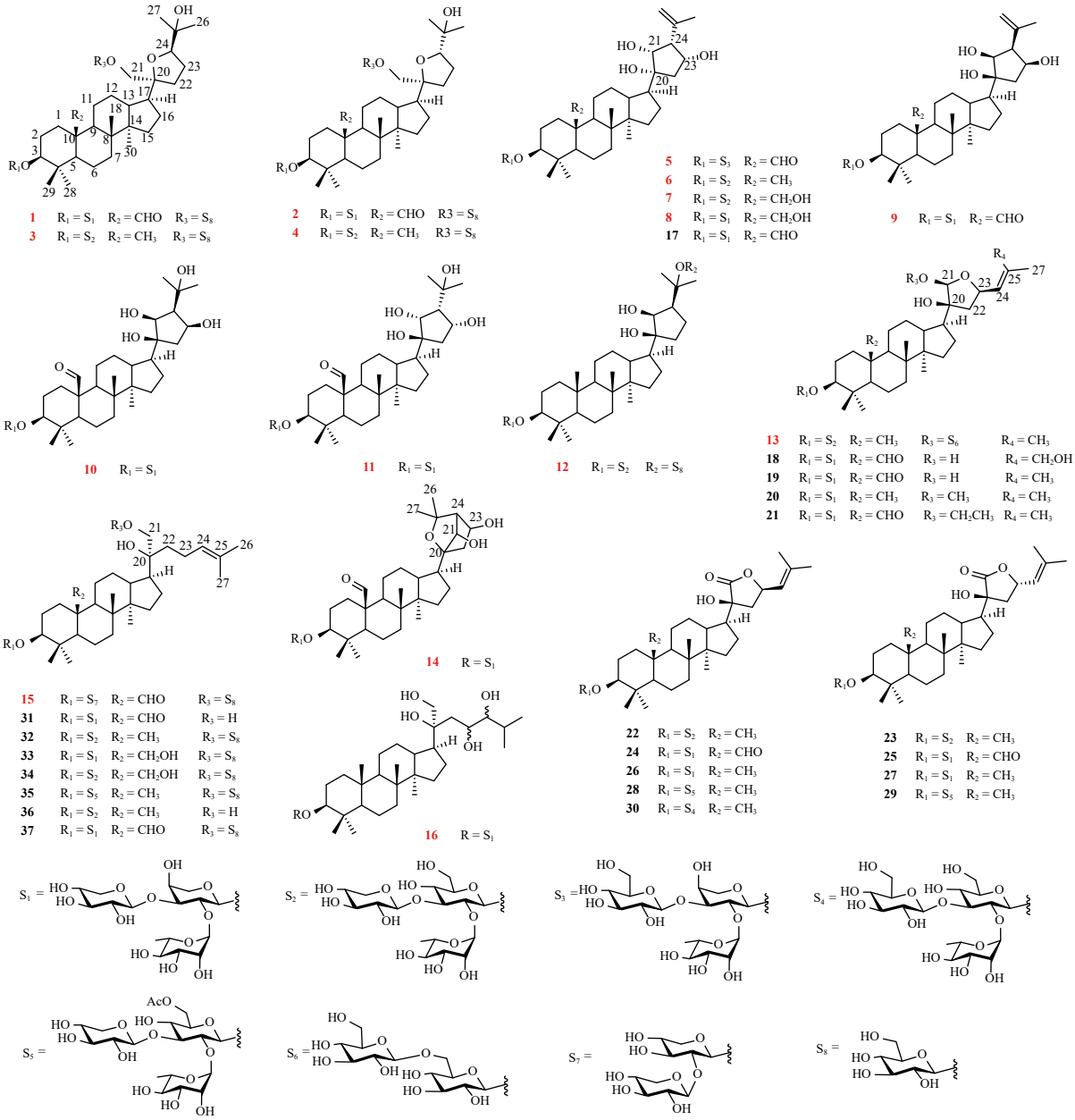

Fig. 1 Structures of compounds 1−37.

be a 20, 24-epoxydammarane saponin. The hydroxy group's position at C-25 was determined by heteronuclear multiple-bond correlation (HMBC) cross-peaks from H-24/H-26/H-27 to the oxygenated carbon C-25 (δ_C 70.5). The presences of *α*-L-arabinopyranosyl, *β*-D-xylopyranosyl, *α*-L-rhamnopyranosyl and *β*-D-glucopyranosyl units was confirmed by acid hydrolysis and high-performance liquid chromatography (HPLC) analysis, alongside the coupling constants of the anomeric protons[14, 15]. The HMBC correlations from H-3 to C-1′ and from H-1‴′ to C-21 determined the glycosylation sites at C-3 and C-21 (Fig. 2), respectively. The sugar chain was elucidated as [*α*-L-rhamnopyranosyl-(1→2)] [*β*-D-xylopyranosyl-(1→3)]-*α*-L-arabinopyranosyl based on the HMBC correlations from δ_H 6.17 (Rha H-1) to δ_C 74.7 (Ara C-2) and from δ_H 5.03 (Xyl H-1) to δ_C 81.7 (Ara C-3). The NOE correlations from H-17 to H-21 and H-17 to H-27, combined with the chemical shifts of C-17, C-20, C-22, and C-23, were instrumental in determining the (20*S*,24*R*) configuration [13]. Consequently, compound **1** was identified as (20*S*, 24*R*)-3*β*,21,25-trihydroxy-19-oxo-20,24-epoxydammarane-3-*O*-[*α*-L-rhamnopyranosyl-(1→2)][*β*-D-xylopyranosyl-(1→3)]-*α*-L-arabinopyranosy-21-*O*-*β*-D-glucopyranoside.

Compound **2**, isolated as a white amorphous powder, exhibited an anionic peak at *m/z* 1061.5502 $[M - H]^-$ (Calcd. for $C_{52}H_{85}O_{22}$, 1061.5532) in HR-ESI-MS spectrum. The acid hydrolysates of **2** yielded L-arabinopyranosyl, D-xylopyranosyl, L-rhamnopyranosyl and D-glucopyranosyl units. The coupling constants of the anomeric protons indicated an *α* configuration for arabinopyranosyl unit (J = 5.8 Hz), a *β* configuration for xylopyranosyl unit (J = 7.8 Hz), an *α* configuration for rhamnopyranosyl (br s) [3] , and a *β* configuration for glucopyranosyl unit (J = 7.8 Hz). The ^{1}H and ^{13}C NMR data for **2** were similar to those of **1**, suggesting a shared structural framework. The distinction between **1** and **2** lies in the configuration of C-24, which was deduced as *S* based on the NOE correlations of H-17 and H-21, H-17 with H-24, and similar chemical shifts to those of gynoside A [13]. Consequently, compound **2** was identified as (20*S*,24*S*)-3*β*,21,25-trihydroxy-19-oxo-20,24-epoxydammarane-3-*O*-[*α*-L-rhamnopyranosyl-(1→2)][*β*-D-xylopyranosyl-(1→3)]-*α*-L-arabinopyranosy-21-*O*-*β*-D-glucopyranoside.

Compound **3** appearing as a white amorphous powder, was determined to have a molecular formula of $C_{53}H_{90}O_{22}$, evidenced by a HR-ESI-MS ion at *m/z* 1077.5839 $[M - H]^-$ (Calcd. for $C_{53}H_{89}O_{22}$, 1077.5845). Acid hydrolysis of **3** produced D-glucopyranosyl, L-rhamnopyranosyl and D-xylopyranosyl units in a ratio of 2 : 1 : 1. The relative configurations of sugar units were determined as *β* for both glucopyranosyl and xylopyranosyl, and *α* for rhamnopyranosyl, based on their coupling constants. The sugar chain was elucidated as [*α*-L-rhamnopyranosyl-(1→2)] [*β*-xylopyranosyl-(1→3)]-D-glucopyranosyl, informed by the HMBC correlations from δ_H 6.49 (Rha H-1) to δ_C 77.0 (Glc C-2) and from δ_H 5.04 (Xyl H-1) to δ_C 88.3 (Glc C-3). The NMR spectrum of the aglycone moiety of **3** was similar to that of compound **1**, with the primary distinction being the absence of the aldehyde group at C-19 [δ_H 0.82 (3H, s); δ_C 16.7], a finding supported by HMBC correlations between H-19 and C-1/C-5/C-9/C-10. Consequently, the structure of **3** was identified as (20*S*, 24*R*)-3*β*,21,25-trihydroxy-20,24-epoxydammarane-3-*O*-[*α*-L-rhamnopyranosyl-(1→2)][*β*-D-xylopyranosyl-(1→3)]-*β*-D-glucopyranosyl-21-*O*-*β*-D-glucopyranoside.

Compound **4**, with a molecular formula of $C_{53}H_{90}O_{22}$ as deduced from its ^{13}C NMR and HR-ESI-MS data (*m/z* 1077.5833 $[M - H]^-$, Calcd. for $C_{53}H_{89}O_{22}$, 1077.5845), was identified. The NMR spectra and acid hydrolysis experiments indicated that the sugar chains at C-3 and C-21 of compound **4** were similar to those of compound **3**. Additionally, the NMR signals of the aglycone in compound **4** were similar to those of compound **2**, but a distinct chemical shift at C-19 [δ_H 0.77 (3H, s); δ_C 16.7] suggested the replacement of the aldehyde group in compound **2** with a methyl group in com-

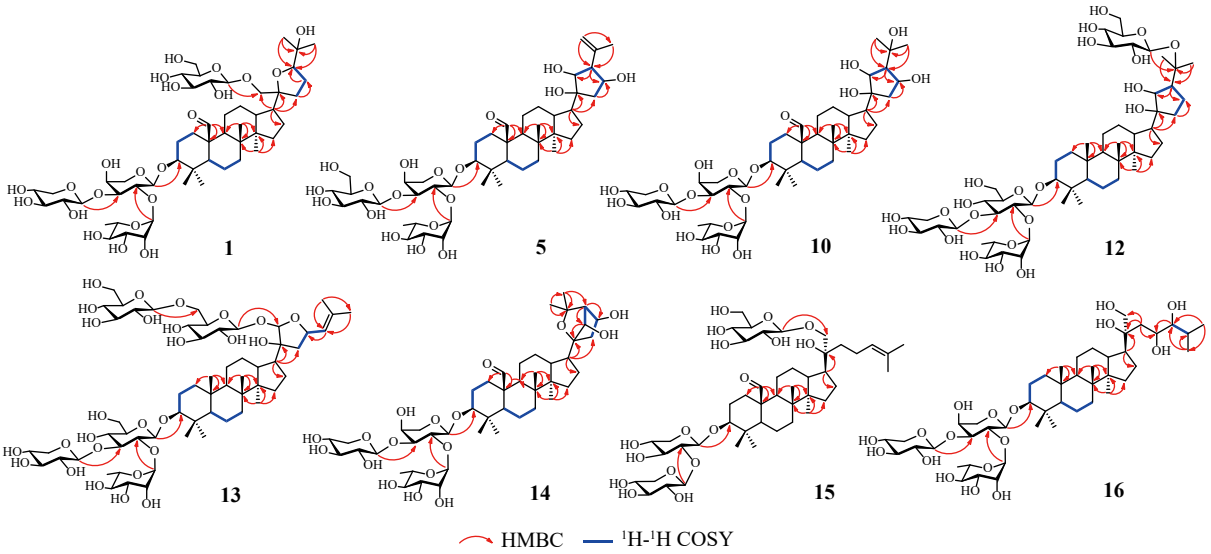

Fig. 2 Key ^{1}H–^{1}H COSY and HMBC correlations of compounds 1, 5, 10, and 12−16.

pound **4**. Consequently, compound **4** was elucidated as (20*S*, 24*S*)-3*β*,21,25-trihydroxy-20,24-epoxydammarane-3-*O*-[*α*-L-rhamnopyranosyl-(1→2)][*β*-D-xylopyranosyl-(1→3)]-*β*-D-glucopyranosyl-21-*O*-*β*-D-glucopyranoside.

Compound **5**, a white amorphous powder, demonstrated a peak at *m/z* 927.4937 $[M - H]^-$ in the HR-ESI-MS, corresponding to a molecular formula $C_{47}H_{76}O_{18}$ (Calcd. for $C_{47}H_{75}O_{18}$, 927.4953). The ^{1}H NMR spectrum displayed signals for five methyl groups (δ_H 0.87, 0.96, 1.11, 1.28 and 2.14, each for 3H), two olefinic protons [δ_H 5.21, 5.33 (each for 1H, s, H-26)], an aldehyde proton [δ_H 10.30 (1H, s, H-29)] and three oxygen-bearing protons [δ_H 3.32 (1H, dd, *J* = 4.1, 12.1 Hz, H-3), 4.41 (1H, d, *J* = 7.1 Hz, H-21), 5.13 (1H, m, H-23)]. The ^{13}C NMR data gave 47 signals, attributing 30 carbons to the aglycone and 17 to the sugar moiety. NMR data of compound **5** closely resembled those of compound **17**, except for the trisaccharide chain at C-3[16]. The attachment sites of three hydroxy groups in the side chain were inferred from observed HMBC correlations (Fig. 2). The presences of *α*-L-arabinopyranosyl, *α*-L-rhamnopyranosyl and *β*-D-glucopyranosyl units was confirmed through acid hydrolysis and and HPLC analysis, along with the coupling constants of anomeric protons [δ_H: 4.84 (1H, d, *J*=6.0 Hz, Ara H-1), 5.12 (1H, d, *J*=8.1 Hz, Glc H-1), 6.20 (1H, brs, Rha H-1)]. The arrangement of sugar chains was further elucidated as [rhamnopyranosyl-(1→2)][glucopyranosyl-(1→3)]-arabinopyranosyl based on the HMBC correlations of δ_H 6.20 (Rha H-1) to δ_C 74.8 (Ara C-2) and δ_H 5.12 (Glc H-1) to δ_C 82.5 (Ara C-3) (Fig. 2). The absolute configuration at C-20 was determined as *R*, in alignment with chemical shifts similar to those of compound **17** [16]. The *R* configuration of C-24 was inferred from the NOE correlation between H-17 and H-24. Additionally, the coupling constant between H-21 and H-24 (*J* = 7.1 Hz) indicated that **5** is a *threo* isomer, thus confirming the *R* configuration of C-21, and the *R* configuration of C-23 was deduced from the NOE correlation between H-21 and H-23. Thus, compound **5** was characterized as (20*R*,21*R*,23*R*,24*R*)-3*β*,20,21,23-tetrahydroxy-19-oxo-21,24-cyclodrammar-25-ene-3-*O*-[*α*-L-rhamnopyranosyl-(1→2)][*β*-D-glucopyranosyl-(1→3)]-*α*-L-arabinopyranoside.

Compound **6** was presented as white amorphous powder with a molecular formula of $C_{47}H_{78}O_{17}$ by a HR-ESI-MS ion at *m/z* 913.4790 $[M - H]^-$ (Calcd. for $C_{47}H_{77}O_{17}$, 913.5161). The 1D and 2D NMR spectra of the aglycone moiety of **6** agreed mostly with those of compound **5.** The main difference is that the aldehyde group at C-19 in **5** was replaced by a methyl group [δ_H 0.81 (3H, s); δ_C 16.6] in **6**, which was also supported by the HMBC correlations between H-19 and C-1/C-9/C-10. Moreover, the trisaccharide moiety was identified as [*α*-L-rhamnopyranosyl-(1→2)] [*β*-D-xylopyranosyl-(1→3)]-*β*-D-glucopyranosyl by good agreement of its NMR data with those of **3** and **4**, as well as the HMBC correlations and acid hydrolysis of **6**. Therefore, the structure of **6** was identified as (20*R*,21*R*,23*R*,24*R*)-3*β*,20,21,23-tetrahydroxy-21,24-cyclodrammar-25-ene-3-*O*-[*α*-L-rhamnopyranosyl-(1→2)][*β*-D-xylopyranosyl-(1→3)]-*β*-D-glucopyranoside.

Compound **7** was assigned a molecular formula of $C_{47}H_{78}O_{18}$, as indicated by its ^{13}C NMR and HR-ESI-MS data (*m/z* 929.5080 $[M - H]^-$; Calcd. for $C_{47}H_{77}O_{18}$, 929.5110). The NMR profile of compound **7** was similar to that of compound **6**, except for a discernible difference in the aglycone at C-19, where the methyl group in **6** underwent hydroxylation in **7**. This modification was evident from the chemical shifts [δ_H 4.17, 4.27 (each for 1H, m, H-19); δ_C 61.6 (C-19)] and supported by HMBC correlations between H-19 and C-1/C-9/C-10. Therefore, the structure of compound **7** was determined as (20*R*,21*R*,23*R*,24*R*)-3*β*,19,20,21,23-pentahydroxy-21,24-cyclodrammar-25-ene-3-*O*-[*α*-L-rhamnopyranosyl-(1→2)][*β*-D-xylopyranosyl-(1→3)]-*β*-D-glucopyranoside.

Compound **8** was obtained as white amorphous powder, with its molecular formula identified as $C_{46}H_{76}O_{17}$, based on HR-ESI-MS at *m/z* 899.4964 $[M - H]^-$ (Calcd. for $C_{46}H_{75}O_{17}$, 899.5004). The NMR data for compound **8** showed a high degree of similarity to those of compound **7**, except for the sugar chain at C-3. The oligosaccharide chain was characterized as [*α*-L-rhamnopyranosyl-(1→2)][*β*-D-xylopyranosyl-(1→3)]-*α*-L-arabinopyranosyl, determined through comparison with the NMR data of compounds **1** and **2**, along with supporting HMBC correlations and acid hydrolysis. Accordingly, the structure of compound **8** was established as as (20*R*,21*R*,23*R*,24*R*)-3*β*,19,20,21,23-pentahydroxy-21,24-cyclodrammar-25-ene-3-*O*-[*α*-L-rhamnopyranosyl-(1→2)][*β*-D-xylopyranosyl-(1→3)]-*α*-L-arabinopyranoside.

Compound **9**, presented as a white amorphous powder, exhibited an anionic peak at *m/z* 897.4805 **[**$M - H]^-$ (Calcd. for $C_{46}H_{73}O_{17}$, 897.4848) in HR-ESI-MS spectrum. The comparison of its 1D and 2D NMR spectroscopic data with those of compound **17** indicated they share the same skeleton, with minor differences in the chemical shifts of the side chain at C-17 due to differing configurations. The absolute configurations of C-20 and C-24 were defined as *S*, based on the chemical shift changes at C-17 (-5.3), C-20 (+1.2), and C-24 (-3.3) between compounds **5** and **9**. [16]. The coupling constant between H-21 and H-24 (*J* = 10.6 Hz) suggested a *threo* isomer, confirming the *S* configuration of C-21. The *S* configuration of C-23 was established by the NOE correlation between H-21 and H-23. Therefore, compound **9**'s structure was elucidated as (20*S*,21*S*,23*S*,24*S*)-3*β*,20,21,23-tetrahydroxy-19-oxo-21,24-cyclodammar-25-ene-3-*O*-[*α*-L-rhamnopyranosyl-(1→2)][*β*-D-xylopyranosyl-(1→3)]-*α*-L-arabinopyranoside.

Compound **10** was purified as a white amorphous powder. The molecular formula was established as $C_{46}H_{76}O_{18}$ based on a negative HR-ESI-MS $[M - H]^-$ ion peak at *m/z* 915.4943. A comparison of the ^{1}H and ^{13}C NMR data between compound **10** and compound **9** revealed that compound **10** is also a 21,24-cyclodammare-type glycoside, bearing the same sugar moieties and sequences, with differences noted in the chemical shifts of H-24 [δ_H 2.37 (1H, t, *J* = 7.2 Hz)]/C-24 (δ_C 59.1), C-25 (δ_C 72.2), and H-26 [δ_H 1.80 (3H,

s)]/C-26 (δ_C 30.5), indicating the presence of a hydroxyl group at C-25. This substitution was corroborated by HMBC correlations from H-26 to C-25 and H-27 to C-25 (Fig. 2). The absolute configurations of C-20 and C-24 were assigned as *S*, matching the chemical shifts with those of compound **9** [16]. Similarly, the coupling constant of H-21 (J = 10.6 Hz) and the NOE correlation of H-21 and H-23 indicated the *S* configuration of C-21 and C-23. Thus, the structure of compound **10** was identified as (20*S*,21*S*,23*S*,24*S*)-3*β*,20,21,23,25-pentahydroxy-19-oxo-21,24-cyclodammar-3-*O*-[*α*-L-rhamnopyranosyl-(1→2)][*β*-D-xylopyranosyl-(1→3)]-*α*-L-arabinopyranoside.

Compound **11**, obtained as a white amorphous powder, suggesting a molecular formula of $C_{46}H_{76}O_{18}$ (Calculated for $C_{46}H_{75}O_{18}$, 915.4953). The NMR spectroscopic profile of compound **11** was similar to that of compound **10**, with a slight difference in the chemical shifts of the side chain at C-17 due to different configurations. The absolute configuration of C-20 was assigned as *S*, by comparing the chemical shifts with those reported in the literature.[16]. Moreover, the similar chemical shifts of C-21, C-23 and C-24 between compound **11** and **5**, the coupling constant of H-21 and the NOE correlation between H-21 and H-23 supported the assignment of the *R* configuration of C-21, C-23 and C-24. Hence, the structure of compound **11** was defined as (20*S*,21*R*,23*R*,24*R*)-3*β*,20,21,23,25- pentahydroxy-19-oxo-21,24-cyclodammar-3-*O*-[*α*-L-rhamnopyranosyl-(1→2)][*β*-D-xylopyranosyl-(1→3)]-*α*-L-arabinopyranoside.

Compound **12** was determined to have a molecular formula of $C_{53}H_{90}O_{22}$, as indicated by its ^{13}C NMR and HR-ESI-MS data (*m/z* 1077.5829 $[M-H]^-$, Calcd for $C_{53}H_{89}O_{22}$, 1077.5845). Acid hydrolysis of **12** yielded D-glucopyranosyl, L-rhamnopyranosyl and D-xylopyranosyl units in a ratio of 2 : 1 : 1. The coupling constants determined the relative configurations of the sugar units as *β* for glucopyranosyl, *β* for xylopyranosyl, and α for rhamnopyranosyl. The sugar chain was elucidated as [*α*-L-rhamnopyranosyl-(1→2)][*β*-D-xylopyranosyl-(1→3)]-D-glucopyranosyl, based on HMBC correlations from δ_H 6.49 (Rha H-1) to δ_C 77.0 (Glc C-2) and from δ_H 5.03 (Xyl H-1) to δ_C 88.2 (Glc C-3). HMBC correlations from H-3 to C-1′ and from H-1‴′ to C-25 identified the glycosylation sites at C-3 and C-25 (Fig. 2), respectively. The NMR spectrum of the aglycone moiety of compound **12** was similar to that of compound **10**, with the primary differences being the absence of the aldehyde group at C-19 [δ_H 0.79 (3H, s); δ_C 16.6] and the hydroxy group at C-23 [δ_H 1.50 (2H, m); δ_C 23.2], which was also supported by the HMBC correlations between H-19 and C-1/C-9/C-10 and H-23 and C-22/C-24. The *S* configuration at C-20 was deduced from the chemical shifts of C-17 and C-20. Additionally, the NOE correlations from H-17 to H-21 and H-21 to H-24 of **12** confirmed the *S* configuration of C-21 and C-24. Therefore, compound **12** was elucidated as (20*S*,21*S*,24*S*)-3*β*,20,21,25-tetrahydroxy-21,24-cyclodammar-3-*O*-[*α*-L-rhamnopyranosyl-(1→2)][*β*-D-xylopyranosyl-(1→3)]-*β*-D-glucopyranosyl-25-*O*-*β*-D-glucopyranoside.

Compound **13** was isolated as a white amorphous powder, with a molecular formula determined as $C_{59}H_{98}O_{27}$, based on HR-ESI-MS ion at *m/z* 1237.6267 $[M-H]^-$ (Calculated for $C_{59}H_{97}O_{27}$, 1237.6217). The 1D NMR spectroscopic data of compound **13** closely resembled those of 3*β*,20*ξ*,21*ξ*-trihydroxy-21,23-epoxydammar-24-ene-3-*O*-[*α*-L-rhamnopyranosyl-(1→2)][*β*-D-xylopyranosyl-(1→3)]-*β*-D-glucopyranoside[16], with the exception of two additional *β*-D-glucopyranosyl groups. These additional sugar units were confirmed by acid hydrolysis and their coupling constants. HMBC correlations (Fig. 2) from δ_H 6.12 (Glc H-1) to δ_C 98.5 (C-21) and from δ_H 5.05 (Glc′ H-1) to δ_C 70.9 (Glc C-6) indicted that the extra disaccharide chain was connected by a 1→6 linkage and attached at C-21. NOE correlations from H-17 to H-21 and H-23 in compound **13** confirmed the *R* configuration of C-21 and C-23. Consequently, the structure of compound **13** was elucidated as (20*S*,21*R*,23*R*)-3*β*,20,21-trihydroxy-21,23-epoxydammar-24-ene-3-*O*-[*α*-L-rhamnopyranosyl-(1→2)][*β*-D-xylopyranosyl-(1→3)]-*β*-D-glucopyranosyl-21-*O*-[*β*-D-glucopyranosyl-(1→6)]-*β*-D-glucopyranoside.

Compound **14** was obtained as a white amorphous powder, with its molecular formula established as $C_{46}H_{74}O_{17}$ through negative-ion HR-ESI-MS data, showing a deprotonated molecular ion at *m/z* 897.4807, and corroborated by ^{13}C NMR data, indicating ten indices of hydrogen deficiency. The types of sugars, trisaccharide sequences, and linkage sites were identified through acid hydrolysis, coupling constants, and 2D NMR analysis. The ^{1}H and ^{13}C NMR spectroscopic data of the aglycone moiety of compound **14** were similar to those of compound **1** but differed in the side chain at C-17. Key distinctions were observed in signals corresponding to the tetrahydropyran ring at C-17 in compound **14**, aligning with those of 3*β*,12*β*,23*S*,24*R*-tetrahydroxy-20*S*,25-epoxydammarane-3-*O*-[*β*-D-xylopyranosyl-(1→2)][*β*-D-xylopyranosyl-(1→6)]-*β*-D-glucopyranoside [17]. The HMBC correlations from H-21 to C-20/C-25 and H-24 to C-20/C-21/C-23/C-25 as well as the ^{1}H-^{1}H COSY correlation from H-21 to H-24 (Fig. 2) , suggested C-21 was linked with C-24 to form an additional ring, contributing to the ten indices of hydrogen deficiency of compound **14**. The placement of two hydroxyl groups on the side chain at C-21 and C-23 was deduced from HMBC correlations from H-24 to C-21 (δ_C 78.5) and from H-22/H-24 to C-23 (δ_C 66.2). Thus, the structure of compound **14** was determined as (20*ξ*,21*ξ*,23*ξ*,24*ξ*)-3*β*,21,23-trihydroxy-19-oxo-21,24-cycly-20,25-epoxydrammar-3-*O*-[*α*-L-rhamnopyranosyl-(1→2)][*β*-D-xylopyranosyl-(1→3)]-*α*-L-arabinopyranoside.

Compound **15** was isolated as a white amorphous powder, and its molecular formula was established as $C_{46}H_{76}O_{17}$, based on a negative HR-ESI-MS $[M-H]^-$ ion peak at *m/z* 899.5041 (Calcd. for $C_{46}H_{75}O_{17}$, 899.5004). The NMR data for compound **15** exhibited high similarity to those of gypenoside XLIX (**37**), except for the sugar chain at

C-3 [18]. The disaccharide chain was identified as *β*-D-xylopyranosyl-(1→2)-*β*-D-xylopyranosyl, as confirmed by acid hydrolysis, along with the coupling constants and HMBC correlations of compound **15**. Therefore, the structure of compound **15** was elucidated as as (20*S*)-3*β*,20,21-trihydroxydammar-19-oxo-24-ene-3-*O*-*β*-D-xylopyranosyl-(1→2)-*β*-D-xylopyranosyl-21-*O*-*β*-D-glucopyranoside.

Compound **16**, also a white amorphous powder, showed an anion peak at *m/z* 903.5293 [M − H]$^-$ (Calcd. for $C_{46}H_{79}O_{17}$, 903.5317) in HR-ESI-MS spectrum. The ^{1}H and ^{13}C NMR data for **16** were akin to those of (3*β*,20*S*)-3,20,21-trihydroxydammar-24-ene-3-*O*-[*α*-L-rhamnopyranosyl-(1→2)][*β*-D-xylopyranosyl-(1→3)]-*α*-L-arabinopyranoside [19],-indicating a shared 3,20,21-trihydroxydammare aglycone core and identical trisaccharide chain. A notable distinction in compound **16** is the substitution of the △$^{24(25)}$ double bond with two hydroxyl groups at C-23 and C-24 [δ_H 4.62 (1H, m, H-23), 3.87 (1H, m, H-24), 2.04 (1H, m, H-25); δ_C 72.8 (C-23), 80.1 (C-24), 26.8 (C-25)], as corroborated by ^{1}H-^{1}H correlation spectroscopy (COSY) correlations between H-23 and H-24 and HMBC correlations from H-24 to C-22/C-23/C-26/C-27. (Fig. 2). The *S* configuration at C-20 was determined based on the chemical shifts of C-17 (δ_C 46.6) and C-20 (δ_C 76.9) [17]. Consequently, the structure of compound **16**'s structure was determined as (20*S*,23*ξ*,24*ξ*)-3*β*,20,21,23,24-pentahydroxydammaraen-3-*O*-[*α*-L-rhamnopyranosyl-(1→2)][*β*-D-xylopyranosyl-(1→3)]-*α*-L-arabinopyranoside.

Additionally, the isolated known compounds **17**–**37** were identified as (20*R*,21*R*,23*R*,24*R*)-3*β*,20,21,23-tetrahydroxy-19-oxo-21,24-cyclodammar-25-ene-3-*O*-[*α*-L-rhamnopyranosyl-(1→2)][*β*-D-xylopyranosyl-(1→3)]-*α*-L-arabinopyranoside (**17**) [16], (20*S*,21*R*,23*R*)-3*β*,20,21,26-tetrahydroxy-19-oxo-21,23-epoxydammar-24-ene-3-*O*-[*α*-L-rhamnopyranosyl-(1→2)][*β*-D-xylopyranosyl-(1→3)]-*α*-L-arabinopyranoside (**18**) [20], gypenoside A (**19**) [16], (20*S*,21*R*,23*R*)-3*β*,20-dihydroxy-21-*O*-methyl-21,23-epoxydammar-24-ene-3-*O*-[*α*-L-rhamnopyranosyl-(1→2)][*β*-D-xylopyranosyl-(1→3)]-*α*-L-arabinopyranoside (**20**) [21], (20*S*,21*R*,23*R*)-21-*O*-ethyl-3*β*,20,21-trihydroxy-19-oxo-21,23-epoxydammar-24-ene-3-*O*-[*α*-L-rhamnopyranosyl-(1→2)][*β*-D-xylopyranosyl-(1→3)]-*α*-L-arabinopyranoside (**21**) [16], (3*β*,20*S*,23*R*)-3,20,23-trihydroxydammar-24-en-21-oic acid-21,23-lactone 3-*O*-[*α*-L-rhamnopyranosyl-(1→2)][*β*-D-xylopyranosyl-(1→3)]-*β*-D-glucopyranoside(**22**)[19], (3*β*,20*S*,23*S*)-3,20,23-trihydroxydammar-24-en-21-oic acid-21,23-lactone-3-*O*-[*α*-L-rhamnopyranosyl-(1→2)][*β*-D-xylopyranosyl-(1→3)]-*β*-D-glucopyranoside (**23**)[19], (3*β*,20*S*,23*S*)-19-oxo-3,20,23-trihydroxydammar-24-en-21-oic acid-21,23-lactone-3-*O*-[*α*-L-rhamnopyranosyl-(1→2)][*β*-D-xylopyranosyl-(1→3)]-*α*-L-arabinopyranoside (**24**) [19], (3*β*,20*S*,23*R*)-19-oxo-3,20,23-trihydroxydammar-24-en-21-oic acid-21,23-lactone-3-*O*-[*α*-L-rhamnopyranosyl-(1→2)][*β*-D-xylopyranosyl-(1→3)]-*α*-L-arabinopyranoside (**25**) [19], (3*β*,20*S*,23*R*)-3,20,23-trihydroxydammar-24-en-21-oic acid-21,23-lactone-3-*O*-[*α*-L-rhamnopyranosyl-(1→2)][*β*-D-xylopyranosyl-(1→3)]-*α*-L-arabinopyranoside (**26**) [19], (3*β*,20*S*,23*S*)-3,20,23-trihydroxydammar-24-en-21-oic acid-21,23-lactone-3-*O*-[*α*-L-rhamnopyranosyl-(1→2)][*β*-D-xylopyranosyl-(1→3)]-*α*-L-arabinopyranoside (**27**) [19], (3*β*,20*S*,23*R*)-3,20,23-trihydroxydammar-24-en-21-oic acid-21,23-lactone-3-*O*-[*α*-L-rhamnopyranosyl-(1→2)][*β*-D-xylopyranosyl-(1→3)]-*β*-D-6-*O*-acetylglucopyranoside (**28**) [19], (3*β*,20*S*,23*S*)-3,20,23-trihydroxydammar-24-en-21-oic acid-21,23-lactone-3-*O*-[*α*-L-rhamnopyranosyl-(1→2)][*β*-D-xylopyranosyl-(1→3)]-*β*-D-6-*O*-acetylglucopyranoside (**29**)[19], (3*β*,20*S*,23*S*)-3,20,23-trihydroxydammar-24-en-21-oic acid-21,23-lactone-3-*O*-[*α*-L-rhamnopyranosyl-(1→2)][*β*-D-glucopyranosyl-(1→3)]-*β*-D-glucopyranoside (**30**) [19], gylongiposide I (**31**) [18], (3*β*,20*S*)-3,20,21-trihydroxydammar-24-ene-3-*O*-[*α*-L-rhamnopyranosyl-(1→2)][*β*-D-xylopyranosyl-(1→3)]-*β*-D-glucopyranosyl-21-*O*-*β*-D-glucopyranoside (**32**) [17], (3*β*,20*S*)-3,19,20,21-tetrahydroxydammar-24-ene-3-*O*-[*α*-L-rhamnopyranosyl-(1→2)][*β*-D-xylopyranosyl-(1→3)]-*α*-L-glucopyranosyl-21-*O*-*β*-D-glucopyranoside (**33**) [17], (3*β*,20*S*)-3,19,20,21-tetrahydroxydammar-24-ene-3-*O*-[*α*-L-rhamnopyranosyl-(1→2)][*β*-D-xylopyranosyl-(1→3)]-*β*-D-glucopyranosyl-21-*O*-*β*-D-glucopyranoside (**34**) [17], (3*β*,20*S*)-3,20,21-trihydroxydammar-24-ene-3-*O*-[*α*-L-rhamnopyranosyl-(1→2)][*β*-D-xylopyranosyl-(1→3)]-*β*-D-6-*O*-acetylglucopyranosyl-21-*O*-*β*-D-glucopyranoside (**35**) [17], (3*β*,20*S*)-3,20,21-trihydroxydammar-24-ene-3-*O*-[*α*-L-rhamnopyranosyl-(1→2)] [*β*-D-xylopyranosyl-(1→3)]-*O*-*β*-D-glucopyranoside (**36**) [18] and gypenoside XLIX (**37**) [18] by comparison of the spectroscopic data with those reported in the literature.

Previous studies have established that dammarane-type saponins from *Gynostemma* possess anti-hypoxic activity. Consequently, 28 isolated compounds in adequate quantities (**1**, **2**, **4**, **6**, **9**, **10**, **12**, **14**–**23**, **26**–**29**, **31**, **32**, and **34**–**37**) underwent evaluation for their protective effects against hypoxia-induced damage in PC12 cells, using salidroside as a positive control. (Fig. 3 and Fig. S1). Hypoxic conditions led to a reduction in PC12 cell viability to 50.9%, in contrast to the 100% viability of normoxic cells. Among the tested saponins, compounds **22**, **23**, **29**, **32**, and **36** demonstrated significant anti-hypoxic effects, enhancing cell viability to 70%−80% in a concentration-dependent manner (3, 10, 30 μmol·L^{-1}). Compounds **26**–**28** and **35** also showed potent protective activities but reduced cell viability at a high concentration of 30 μmol·L^{-1}. The preliminary structure-activity relationship suggested that gypenosides featuring a 20,23-dihydroxydammar-24-en-21-oic acid-21,23-lactone moiety exhibited the most potent anti-hypoxic activity. All such compounds (**22**, **23**, **26**–**29**) were effective in preventing hypoxia-induced injury in PC12 cells. Additionally, an increased number of sugar moieties appeared to negatively affect the protective effects, aligning with observations in ginsenosides.[22].

Compounds **22** and **36**, as two representative saponin types from *G. longipes*, showed the most promising anti-hypoxic activities and were selected for further investigation into their protective mechanisms. As depicted in Fig. 4, hypoxic

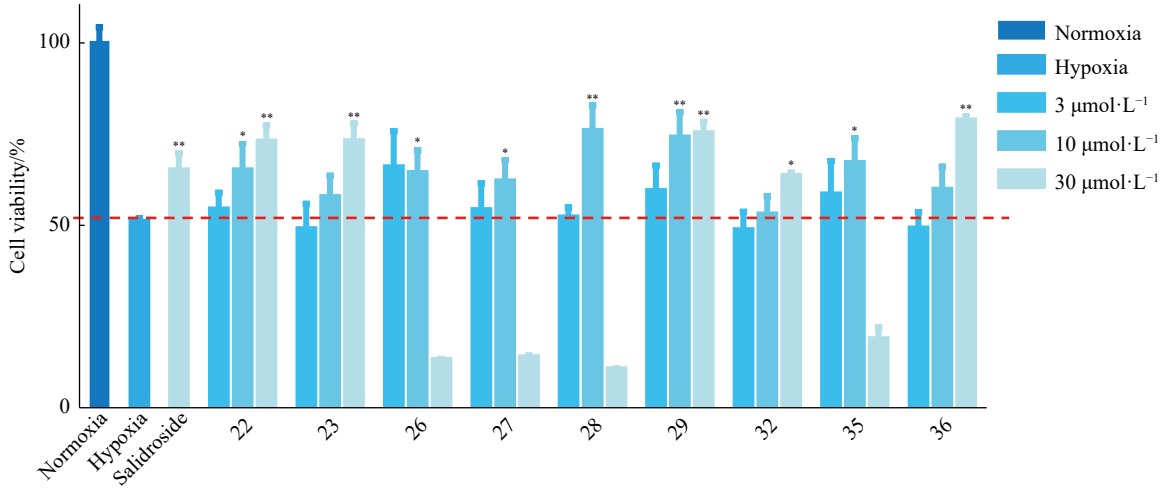

Fig. 3 The activity of the bioactive compounds on the cell viability of hypoxic-induced PC12 cells. All results were expressed as mean ± SD (n = 3). $^{**}P < 0.01$, $^{*}P < 0.05$ *vs* the hypoxia group.

conditions significantly increased the apoptosis rate in PC12 cells from 0.6% under normoxia to 48.5%. Treatment with compounds **22** and **36** resulted in a notable decrease in the percentage of apoptotic cells to 40.7%, 29.2%, and 23.7% for compound **22**, and 36.2%, 31.9%, and 26.0% for compound **36**, at concentrations of 3, 10, and 30 μmol·L^{-1}, respectively (Fig. 4 and Fig. S2). These findings suggest that the anti-hypoxic mechanism of these saponins may involve the reduction of apoptosis to improve cell viability.

Oxidative stress plays a pivotal role in mediating alterations induced by hypoxia. Under hypoxic conditions, the level of lactate dehydrogenase (LDH) in PC12 cells significantly increased, indicating cytosolic leakage of LDH. Treatment with compounds **22** and **36** markedly reduced LDH release, outperforming salidroside. Likewise, the elevated malondialdehyde (MDA) levels induced by hypoxia were significantly diminished under the intervention of these two saponins. In contrast, treatments with compounds **22** and **36** resulted in a noticeable increase in superoxide dismutase (SOD) levels (Fig. 5). These results suggest that the saponins could mitigate oxidative stress, thereby preventing hypoxia-induced injuries.

Experimental

General experimental procedures

NMR spectra were acquired using a Bruker Avance III 600 MHz spectrometer (Bruker Corporation, Germany), ensuring high precision in structural elucidation. High-resolution electrospray ionization mass spectrometry (HR-ESI-MS) data were collected on a Waters Synapt MS spectrometer (Waters Corporation, UK), facilitating accurate mass determination of the isolated compounds. Semi-preparative HPLC was conducted using a Hanbon Newstyle NP7000 pump (Hanbon Sci. & Tech., China) coupled with a Shodex RID 101 refractive index detector (Showa Denko K.K., Japan), employing both a XUnion C_{18} (250 mm × 10.0 mm, 5 μm) and a Phenomenex Kinetex C_{18} column (150 mm × 10.0 mm, 5 μm) for separation. Analytical HPLC analyses were performed on a Waters 2695 system (Waters Corporation, UK) equipped with an Alltech 2000 evaporative light scattering detector (Alltech Associates, Inc., UK), using a XUnion C_{18} (250 mm × 4.6 mm, 5 μm) and Phenomenex Kinetex C_{18} column (150 mm × 10.0 mm, 2.6 μm), enabling precise component analysis and purity assessment. Column chromatography (CC) utilized Silica gel (200–300 mesh, Qingdao Marine Chemical Co., Ltd., China), MCI gel (50 μm, Mitsubishi Chemical Corporation, Japan), and macroporous resin D101 (Tianjin Haoju Resin Technology Co., Ltd., China), ensuring effective fractionation and isolation of compounds. Thin-layer chromatography (TLC) was conducted on silica gel GF_{254} plates (Tianjin Silida Technology Co., Ltd., China) for rapid qualitative analysis. Analytical and HPLC-grade solvents, ensuring consistency and reliability in all chromatographic separations, were employed throughout the isolation process.

Plant materials

The dry rhizomes of *Gynostemma longipes* C. Y. Wu were collected from Pingli County, Ankang City, Shaanxi Province, and were identified by one of the authors, Prof. Bao-Lin Guo. A voucher specimen (No.151010) has been deposited in the author's laboratory.

Extraction and isolation

The isolation and purification protocol for compounds from *G. longipes* involved a meticulous extraction process starting with 12.0 kg of the dried plant material. This material was powdered and extracted with water three times, each for 1.5 hours. The filtrates were concentrated under reduced pressure and subjected to macroporous resin D101 column chromatography, eluting first with water and then with 80% aqueous methanol. The methanol fraction was collected and further concentrated to obtain a crude extract weighing 600 g, containing the total saponins of *G. longipes*. This crude extract was subsequently fractionated using 30% and 50% acetonitrile solutions to produce fractions A and B.

Fraction A underwent further separation through MCI medium-pressure liquid chromatography (MPLC), using a gradient of acetonitrile-water (MeCN-H_2O) mixtures (20 : 80, 50 : 50, 80 : 20, *V/V*), resulting in five subfractions (A1–A5). The A2 subfraction, identified to contain target polar saponins through UPLC-Q-TOF MS analysis, was subjected to silica gel column chromatography, eluted with a gradient of chloroform-methanol (8 : 1, 6 : 1, 3 : 1, *V/V*), yielding twelve subfractions (A2-1−A2-12). Selective subfractions were further purified using preparative HPLC. Specifically, A2-3 underwent purification with a MeCN-H_2O (24 : 76, *V/V*) mobile phase to yield compounds **9** (12 mg) and **17** (416 mg). Compound **14** (10 mg) was isolated from A2-5 using the same mobile phase. A2-6 was fractionated *via* MCI column chromatography with MeOH-H_2O gradients, producing subfractions A2-6a to A2-6h. A2-6c was further purified by preparative HPLC (MeCN-H_2O, 26 : 74, *V/V*) to afford compounds **5** (8 mg), **10** (2 mg), and **11** (14 mg). Compound **16** (7 mg) was isolated from A2-6f using a preparative HPLC mobile phase of MeCN-H_2O (23 : 77, *V/V*). A2-7 was subjected to MCI chromatography and further fractionation, with A2-7b purified *via* preparative HPLC (MeCN-H_2O, 26 : 74, *V/V*) to yield compounds **1** (15 mg), **7** (4 mg), **8** (5 mg), and **18** (30 mg). Compound **3** (4 mg) was isolated from A2-7d using a MeCN-H_2O (28 : 72, *V/V*) mobile phase. A2-9, separated over a C_{18} column with MeOH-H_2O (55 : 45, *V/V*), produced compound **4** (12 mg) and **12** (27 mg). A2-9c was further purified by preparative HPLC (MeCN-H_2O, 26 : 74, *V/V*) to yield compound **2** (9 mg). Compound **13** (6 mg) was isolated from A2-11 using a preparative HPLC mobile phase of MeCN-H_2O (28 : 72, *V/V*).

Fraction B underwent a sequential and detailed purification process, beginning with MPLC over MCI gel, using a gradient of acetonitrile-water (MeCN-H_2O) (20 : 80, 50 : 50, 80 : 20, *V/V*) to divide it into five subfractions (B1–B5). Subfraction B4 was then refined *via* C_{18} column chromatography,

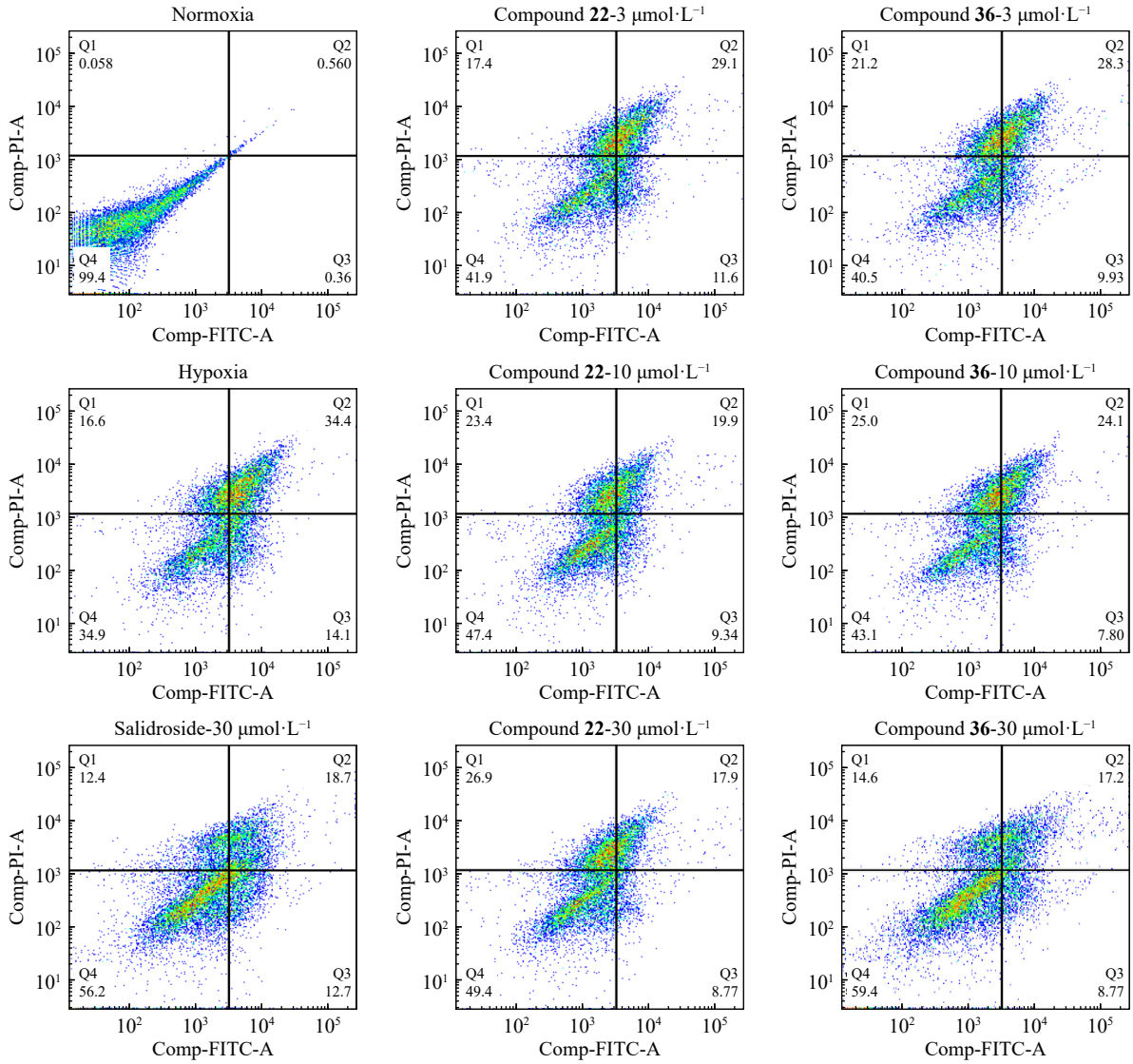

Fig. 4 Effects of compounds 22 and 36 on apoptosis in PC12 cells under hypoxia conditions.

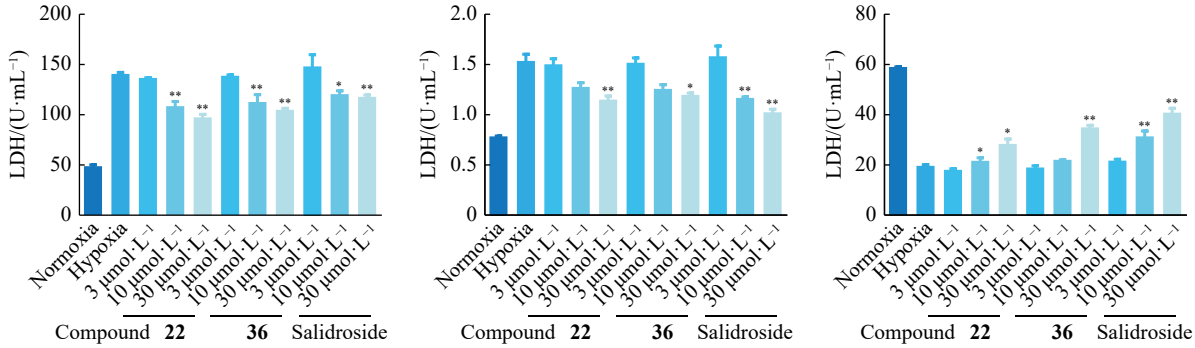

Fig. 5 Effects of compounds 22 and 36 on the levels of LDH, MDA and SOD. All results were expressed as mean ± SD (n = 3). $^{**}P < 0.01$, $^{*}P < 0.05$ *vs* the hypoxia group.

eluted with MeCN-H_2O (35 : 65, *V/V*), yielding two further fractions (B4-1 and B4-2). B4-1 underwent additional C_{18} chromatography, this time with MeCN-H_2O (30 : 70, *V/V*), resulting in four fractions (B4-1a to B4-1d). Among these, B4-1b was purified using preparative HPLC with a mobile phase of MeCN-H_2O (28 : 72, *V/V*), isolating compounds **6** (30 mg) and **34** (30 mg). B4-1d was similarly processed by preparative HPLC (MeCN-H_2O, 29 : 71, *V/V*) to yield compounds **15** (25 mg), **33** (13 mg), and **37** (200 mg). Further fractionation of B4-2 *via* C_{18} chromatography with MeCN-H_2O (35 : 65, *V/V*) produced five subfractions (B4-2a to B4-2e). From these, compound **19** (500 mg) was isolated from B4-2a using preparative HPLC (MeCN-H_2O, 30 : 70, *V/V*). B4-2b was further refined by preparative HPLC (MeCN-H_2O, 33 : 67, *V/V*) to obtain compounds **31** (33 mg) and **35** (30 mg), and B4-2c was processed (MeCN-H_2O, 35 : 65, *V/V*) to separate compounds **32** (40 mg), **24** (10 mg), **25** (11 mg), and **30** (14 mg). B4-2d yielded compounds **22** (304 mg), **23** (260 mg), **26** (28 mg), **27** (17 mg), and **36** (23 mg) upon purification with preparative HPLC (MeCN-H_2O, 40 : 60, *V/V*), and B4-2e facilitated the isolation of compounds **20** (26 mg) and **21** (30 mg) under a preparative HPLC regime (MeCN-H_2O, 42 : 58, *V/V*). Post-evaporation of the organic solvents, the extract from fraction B5 was subjected to sequential partitioning with petroleum ether and ethyl acetate. The ethyl acetate fraction was chromatographed over silica gel using a gradient elution of chloroform: methanol: H_2O (85 : 15 : 1, *V/V*), dividing it into four fractions (B5-E1 to B5-E4). Notably, B5-E3 underwent further purification by preparative HPLC (MeCN-H_2O, 45 : 55, *V/V*) to yield compounds **28** (160 mg) and **29** (35 mg). This rigorous and step-wise purification strategy was instrumental in isolating and identifying a diverse array of compounds, highlighting the complex phytochemistry of *Gynostemma longipes* and contributing valuable insights into its potential bioactive components.

(20S,24R)-3β,21,25-trihydroxy-19-oxo-20,24-epoxydammarane-3-O-[α-L-rhamnopyranosyl-(1→2)][β-D-xylopyranosyl-(1→3)]-α-L-arabinopyranosy-21-O-β-D-glucopyranoside (**1**): white amorphous powder; ^{1}H and ^{13}C NMR data, see Table 1; HR-ESI-MS *m/z* 1061.5546 $[M - H]^-$ (Calcd. for $C_{52}H_{85}O_{22}$, 1061.5532).

(20S,24S)-3β,21,25-trihydroxy-19-oxo-20,24-epoxydammarane-3-O-[α-L-rhamnopyranosyl-(1→2)][β-D-xylopyranosyl-(1→3)]-α-L-arabinopyranosy-21-O-β-D-glucopyranoside (**2**): white amorphous powder; ^{1}H and ^{13}C NMR data, see Table 1; HR-ESI-MS *m/z* 1061.5502 $[M - H]^-$ (Calcd. for $C_{52}H_{85}O_{22}$, 1061.5532).

(20S,24R)-3β,21,25-trihydroxy-20,24-epoxydammarane-3-O-[α-L-rhamnopyranosyl-(1→2)][β-D-xylopyranosyl-(1→3)]-β-D-glucopyranosyl-21-O-β-D-glucopyranoside (**3**): white amorphous powder; ^{1}H and ^{13}C NMR data, see Table 1; HR-ESI-MS *m/z* 1077.5839 $[M - H]^-$ (Calcd. for $C_{53}H_{89}O_{22}$, 1077.5845).

(20S,24S)-3β,21,25-trihydroxy-20,24-epoxydammarane-3-O-[α-L-rhamnopyranosyl-(1→2)][β-D-xylopyranosyl-(1→3)]-β-D-glucopyranosyl-21-O-β-D-glucopyranoside (**4**): white amorphous powder; ^{1}H and ^{13}C NMR data, see Table 1; HR-ESI-MS *m/z* 1077.5833 $[M - H]^-$ (Calcd. for $C_{53}H_{89}O_{22}$, 1077.5845).

(20R,21R,23R,24R)-3β,20,21,23-tetrahydroxy-19-oxo-21,24-cyclodrammar-25-ene-3-O-[α-L-rhamnopyranosyl (1→2)][β-D-glucopyranosyl(1→3)]-α-L-arabinopyranoside (**5**): white amorphous powder; ^{1}H and ^{13}C NMR data, see Tables 2 and 3; HR-ESI-MS *m/z* 927.4937 $[M - H]^-$ (Calcd. for $C_{47}H_{75}O_{18}$, 927.4953).

(20R,21R,23R,24R)-3β,20,21,23-tetrahydroxy-21,24-cyclodrammar-25-ene-3-O-[α-L-rhamnopyranosyl-(1→2)][β-D-xylopyranosyl-(1→3)]-β-D-glucopyranoside (**6**): white amorphous powder; ^{1}H and ^{13}C NMR data, see Tables 2 and 3; HR-ESI-MS *m/z* 913.4790 $[M - H]^-$ (Calcd. for $C_{47}H_{77}O_{17}$, 913.5161).

(20R,21R,23R,24R)-3β,19,20,21,23-pentahydroxy-21,24-cyclodrammar-25-ene-3-O-[α-L-rhamnopyranosyl-(1→2)][β-D-xylopyranosyl-(1→3)]-β-D-glucopyranoside (**7**): white amorphous powder; ^{1}H and ^{13}C NMR data, see Tables 2 and 3; HR-ESI-MS *m/z* 929.5080 $[M - H]^-$ (Calcd. for $C_{47}H_{77}O_{18}$, 929.5110).

(20R,21R,23R,24R)-3β,19,20,21,23-pentahydroxy-21,24-cyclodrammar-25-ene-3-O-[α-L-rhamnopyranosyl(1→2)][β-D-xylopyranosyl(1→3)]-α-L-arabinopyranoside (**8**): white amorphous powder; ^{1}H and ^{13}C NMR data, see Tables 2 and 3; HR-ESI-MS *m/z* 899.4964 $[M - H]^-$ (Calcd. for $C_{46}H_{75}O_{17}$, 899.5004).

(20S,21S,23S,24S)-3β,20,21,23-tetrahydroxy-19-oxo-

Table 1 ^{1}H NMR and ^{13}C NMR data of compounds 1–4 in pyridine-d_5 (δ in ppm, J in Hz).

Position	1		2		3		4	
	δ_H	δ_C	δ_H	δ_C	δ_H	δ_C	δ_H	δ_C
1	0.72 m, 2.64 dd (3.0, 7.7)	33.6	0.66 m, 2.59 dd (3.1, 7.6)	33.6	0.84 m, 1.46 m	39.7	0.84 m, 1.40 m	39.7
2	2.08 m	27.6	2.08 m	27.6	1.28 m, 2.31 m	26.9	2.28 m	26.9
3	3.34 dd (4.0, 12.1)	87.1	3.31 dd (4.0, 12.1)	87.1	3.40 dd (4.1, 12.0)	88.9	3.88 dd (4.0, 11.8)	88.9
4		40.4		40.4		39.7		39.7
5	1.17 m	54.8	1.14 m	54.9	0.73 d (11.4)	56.7	0.70 d (11.6)	56.7
6	1.66 m, 1.92 m	17.7	1.66 m, 1.90 m	17.7	1.62 m, 1.65 m	18.5	1.62 m, 1.65 m	18.5
7	1.36 m, 1.64 m	34.7	1.35 m, 1.62 m	34.7	1.25 m	35.7	1.22 m	35.7
8		40.1		40.1		40.7		40.7
9	1.68 m	53.0	1.64 m	53.0	1.26 m	51.2	1.24 m	51.1
10		52.8		52.8		37.1		37.0
11	1.15 m, 1.74 m	22.7	1.12 m, 1.63 m	22.3	1.46 m	22.2	1.34 m, 2.00 m	21.9
12	1.72 m	26.0	1.86 m	26.0	1.66 m	26.1	1.63 m	26.0
13	1.79 m	42.5	1.79 m	42.4	1.89 m	42.7	1.89 m	42.6
14		49.9		49.9		50.1		50.3
15	1.10 m, 1.46 m	32.4	1.11 m, 1.53 m	32.3	1.05 m	32.1	1.07 m, 1.58 m	32.0
16	1.68 m	27.5	1.13 m, 1.68 m	27.6	2.13 m	27.6	2.22 m	27.9
17	2.22 m	45.4	2.29 m	45.1	2.21 m	45.7	2.30 m	45.4
18	1.11 s	16.0	1.09 s	16.0	0.99 s	15.7	0.97 s	15.7
19	10.35 s	205.7	10.31 s	205.7	0.82 s	16.7	0.77 s	16.7
20		88.5		88.1		88.7		88.7
21	3.70 m, 4.07 m	76.4	3.69 m, 4.25 m	74.6	3.74 m, 3.76 m	76.4	3.75 m	74.6
22	1.85 m, 2.07 m	30.4	1.76 m, 2.07 m	31.3	2.11 m	30.5	1.81 m, 2.12 m	31.5
23	1.84 m, 2.30 m	27.1	2.00 m	27.2	1.87 m	27.2	2.04 m	27.2
24	3.84 m	87.7	4.26 m	86.0	3.93 m	87.4	4.30 m	86.0
25		70.5		71.1		70.6		70.6
26	1.47 s	28.3	1.40 s	26.9	1.51 s	28.3	1.43 s	26.9
27	1.25 s	26.2	1.45 s	26.7	1.28 s	26.3	1.48 s	26.7
28	1.27 s	26.4	1.25 s	26.4	1.27 s	27.9	1.25 s	27.8
29	0.91 s	16.6	0.91 s	16.6	1.21 s	16.7	1.18 s	16.9
30	0.92 s	17.1	0.88 s	17.1	0.90 s	16.9	0.90 s	16.8
C-3-*O*	Ara		Ara		Glc		Glc	
1′	4.91 d (5.6)	104.7	4.90 m	104.7	4.93 d (7.6)	105.1	4.93 d (7.7)	105.0
2′	3.95 m	74.7	3.94 m	74.6	4.27 m	77	3.74 m	77.0
3′	4.30 m	81.7	4.29 m	81.8	4.20 m	88.3	4.23 m	88.3
4′	4.48 brs	68.5	4.48 brs	68.5	4.03 m	69.8	4.03 m	69.8
5′	3.82 m, 4.28 m	65.2	3.81 d (9.8), 4.29 m	65.1	4.23 m	78.1	3.93 m	78.1
6′					4.30 m, 4.54 m	62.6	4.31 m, 4.54 m	62.6
	Rha		Rha		Rha		Rha	
1″	6.17 brs	102.1	6.17 brs	102.1	6.49 brs	101.8	6.48 brs	101.8
2″	4.60 m	72.6	4.59 m	72.6	4.62 m	72.6	4.62 m	72.6
3″	4.76 m	72.5	4.76 m	72.5	4.83 m	72.5	4.83 m	72.5
4″	4.30 m	73.9	4.30 m	73.9	4.33 m	73.9	4.33 m	73.9
5″	4.59 m	70.1	4.58 m	70.1	4.79 m	69.9	4.79 m	69.9
6″	1.62 d (6.1)	18.6	1.62 d (6.1)	18.6	1.72 d (6.2)	18.7	1.71 d (6.1)	18.7
	Xyl		Xyl		Xyl		Xyl	
1‴	5.03 d (7.4)	105.3	5.02 m	105.3	5.04 d (7.7)	104.9	5.02 m	104.9
2‴	4.66 t (7.1)	74.5	4.66 t (6.4)	74.5	3.98 m	74.9	3.99 m	74.9
3‴	4.12 m	77.8	4.11 m	77.8	4.04 m	78.3	4.11 m	78.3
4‴	4.13 m	70.9	4.12 m	70.9	4.12 m	70.7	4.13 m	70.7
5‴	3.68 m, 4.33 m	67.1	3.68 m, 4.32 m	67.0	3.72 m, 4.28 m	67.3	3.72 m, 4.28 m	67.3
C-21-*O*	Glc		Glc		Glc		Glc	
1⁗	4.84 d (7.8)	105.0	4.92 m	105.7	4.86 d (7.8)	105.1	4.91 d (7.6)	105.6
2⁗	4.04 t (8.3)	75.0	4.06 t (8.2)	75.2	4.06 m	75.1	4.07 m	75.2
3⁗	4.22 m	78.6	4.27 m	78.7	4.21 m	78.8	4.27 m	78.7
4⁗	4.21 m	71.7	4.22 m	71.9	4.18 m	71.7	4.23 m	71.9
5⁗	3.95 m	78.8	4.01 m	78.6	4.23 m	78.7	4.01 m	78.6
6⁗	4.35 m, 4.57 m	62.9	4.40 m, 4.61 m	63.0	4.36 m, 4.60 m	63.0	4.41 m, 4.60 m	63.0

Table 2 ^{1}H NMR data of compounds 5–11 in pyridine-d_5 (δ in ppm, J in Hz).

Position	5	6	7	8	9	10	11
	δ_H	δ_H	δ_H	δ_H	δ_H	δ_H	δ_H
1	0.71 m, 2.62 m	0.98 m, 1.63 m	0.87 m, 2.52 m	0.91 m, 2.60 m	0.70 m, 2.64 m	0.70 m, 2.63 m	0.74 m, 2.65 m
2	2.08 m	2.19 m, 1.76 m	1.88 s	1.88 s	1.35 m, 2.08 m	2.09 m	2.09 m
3	3.32 dd (4.1, 12.1)	3.43 dd (4.0, 11.8)	3.54 dd (4.3, 11.8)	3.42 dd (4.4, 11.8)	3.33 dd (4.1, 11.8)	3.32 dd (4.1, 11.8)	3.34 dd (4.0, 12.0)
4							
5	1.18 m	0.81 d (11.7)	0.98 m	0.99 m	1.17 m	1.17 m	1.16 m
6	1.90 s	1.53 m, 1.44 m	1.54 m	1.53 m	1.90 s	1.90 m	1.90 m
7	1.36 m, 1.65 m	1.22 m, 1.49 m	1.33 m, 1.63 m	1.36 m, 1.67 m	1.34 m, 1.65 m	1.33 m, 1.64 m	1.35 m, 1.64 m
8							
9	1.69 m	1.33 m	1.50 m	1.54 m	1.71 m,	1.70 m	1.70 m
10							
11	1.68 m	1.23 m, 1.47 m	1.86 m	2.20 m	1.22 m, 1.76 m	1.19 m, 1.72 m	1.09 m, 1.68 m
12	1.90 m	1.84 m, 1.90 m	2.25 m, 2.40 m	2.18 m, 2.26 m	1.87 m, 2.01 s	1.83 m, 1.98 s	2.62 m
13	2.01 m	2.06 m	2.20 m	2.21 m	1.91 m	1.91 m	2.09 m
14							
15	1.15 m, 1.58 m	1.09 m, 1.61 m	1.17 m, 1.72 m	1.17 m, 1.73 m	1.13 m, 1.55 d (10.1)	1.12 m, 1.51 d (10.3)	1.16 m, 1.64 m
16	1.68 m, 2.24 m	1.42 m, 2.13 m	2.35 m	2.33 m	1.69 m, 2.62 m	1.69 m	1.70 m
17	2.02 m	2.01 m	2.10 m	2.10 m	2.25 m, 2.60 m	2.24 m, 2.50 m	2.66 m
18	1.11 s	0.93 s	1.31 s	1.32 s	1.11 s	0.84 s	1.10 s
19	10.30 s	0.81 s	4.17 m, 4.27 m	4.19 m, 4.29 m	10.32 s	10.31 s	10.31 s
20							
21	4.41 d (7.1)	4.42 d (7.2)	4.48 d (7.3)	4.48 d (7.3)	4.70 d (10.6)	4.86 d (10.6)	4.64 d (10.9)
22	2.08 m, 2.67 m	2.09 m, 2.68 dd (6.8,12.8)	2.12 s, 2.70 dd (6.7, 12.7)	2.12 s, 2.70 dd (6.7, 12.7)	2.28 m	2.26 m	2.16 m
23	5.13 m	5.09 m	5.12 s	5.13 m	4.61 m	4.84 m	5.22 m
24	2.94 t (8.6)	2.94 t (8.5)	2.96 t (8.0)	2.96 t (7.9)	3.11 dd (4.5, 10.6)	2.40 dd (4.9, 10.6)	2.37 t (7.2)
25							
26	5.21 s, 5.33 s	5.30 brs	5.20 s, 5.30 s	5.20 s, 5.33 s	5.41 s, 5.23 s	1.73 s	1.80 s
27	2.14 s	2.10 s	2.12 s	2.12 s	2.01 s	1.83 s	1.82 s
28	1.28 s	1.23 s	1.32 s	1.27 s	1.26 s	1.25 s	1.25 s
29	0.96 s	1.15 s	1.32 s	1.27 s	0.96 s	1.10 s	0.94 s
30	0.87 s	0.94 s	1.00 s	1.03 s	0.87 s	0.94 s	0.84 s
C-3-*O*	Ara	Glc	Glc	Ara	Ara	Ara	Ara
1′	4.84 d (6.0)	4.83 d (7.4)	4.96 d (7.4)	4.98 d (5.5)	4.90 d (5.6)	4.90 d (5.6)	4.90 d (5.7)
2′	3.97 m	4.21 m	4.24 m	3.94 t (7.7)	3.94 t (7.7)	3.94 t (7.1)	3.94 t (7.7)
3′	4.32 m	4.15 m	4.20 m	4.33 m	4.30 m	4.30 m	4.30 m
4′	4.31 m	3.84 t (9.2)	4.02 m	4.50 m	4.49 brs	4.49 brs	4.49 brs
5′	3.75 d (10.1)	3.98 m	3.93 m	3.85 m, 4.33 m	3.82 d (9.8), 4.29 m	3.82 d (9.7), 4.30 m	3.82 d (10.3), 4.29 m
6′		4.71 m, 4.83 m	4.15 m, 4.29 m				
	Rha	Rha	Rha	Rha	Rha	Rha	Rha
1″	6.20 brs	6.44 brs	6.46 brs	6.16 s	6.17 s	6.16 brs	6.77 brs
2″	4.60 m	4.79 m	4.61 m	4.62 m	4.60 m	4.61 m	4.61 m
3″	4.76 m	4.59 m	4.82 m	4.76 m	4.76 m	4.76 m	4.77 m
4″	4.30 m	4.29 m	4.31 m	4.30 m	4.30 m	4.30 m	4.30 m
5″	4.78 m	4.72 m	4.79 m	4.62 m	4.61 m	4.59 m	4.59 m
6″	1.61 d (6.1)	1.69 d (6.2)	1.65 d (6.2)	1.62 d (6.2)	1.62 d (6.2)	1.62 d (6.2)	1.62 d (6.1)
	Glc	Xyl	Xyl	Xyl	Xyl	Xyl	Xyl
1‴	5.12 d (8.1)	5.01 d (7.5)	5.03 d (7.7)	5.03 d (7.4)	5.03 brs	5.04 m	5.04 brs
2‴	4.65 t (7.2)	3.98 m	3.98 m	4.96 t (5.9)	4.66 t (6.9)	4.66 t (7.1)	4.67 m
3‴	4.12 m	4.09 m	4.12 m	4.11 m	4.11 m	4.12 m	4.11 m
4‴	4.17 m	4.13 m	4.13 m	4.13 m	4.12 m	4.13 m	4.13 m
5‴	4.20 m	3.70 t (10.7), 4.29 m	3.71 t (10.9), 4.27 m	3.68 t (11.0), 4.32 m	3.68 t (10.9), 4.32 m	3.67 t (11.0), 4.33 m	3.68 t (10.7), 4.33 m
6‴	4.33 m, 4.52 m						

Table 3 ^{13}C NMR data of compounds 5–11 in pyridine-d_5 (δ in ppm).

Position	5	6	7	8	9	10	11
	δ_C	δ_C	δ_C	δ_C	δ_C	δ_C	δ_C
1	33.6	39.7	35.1	34.9	33.6	33.6	33.6
2	27.6	26.9	25.6	25.6	27.7	27.7	27.8
3	87.1	88.9	89.2	88.7	87.1	87.1	87.1
4	40.4	39.6	39.7	39.8	40.4	40.4	40.4
5	54.9	56.6	57.4	57.3	54.9	54.9	54.8
6	17.7	18.4	18.3	18.3	17.7	17.7	17.7
7	34.7	35.7	36.3	36.3	34.7	34.7	34.6
8	40.1	40.6	41.0	41.0	40.1	41.0	41.0
9	52.8	51.0	53.1	53.2	53.0	53.0	52.9
10	52.8	37.0	42.1	42.2	52.8	52.8	52.8
11	22.2	21.7	24.8	24.8	22.2	22.4	22.3
12	25.5	25.5	27.8	27.6	25.6	25.6	25.8
13	42.4	42.7	43.2	43.2	44.0	43.9	42.0
14	50.2	50.4	50.8	50.8	50.2	50.2	50.6
15	31.9	31.5	32.0	32.0	32.2	32.1	32.1
16	27.3	27.4	28.6	28.7	27.6	27.6	27.6
17	50.2	50.3	50.2	50.3	44.9	45.4	47.8
18	16.0	15.7	16.1	16.1	16.0	16.4	16.0
19	205.5	16.6	61.6	61.6	205.6	205.6	205.6
20	80.5	80.6	80.8	80.8	81.7	81.8	81.7
21	76.9	76.1	76.1	76.1	76.0	75.5	77.2
22	47.2	47.0	47.0	47.1	48.3	48.2	48.1
23	71.5	71.6	71.6	71.6	69.7	70.5	70.7
24	60.3	60.3	60.3	60.3	57.0	56.4	59.1
25	144.6	144.5	144.7	144.6	144.1	72.2	72.5
26	112.8	112.8	112.7	112.7	112.4	30.7	30.5
27	23.5	23.5	23.5	23.5	23.5	29.9	29.9
28	26.4	27.9	28.5	28.4	26.4	26.4	26.4
29	16.6	16.9	17.1	17.1	16.4	16.0	16.4
30	17.2	16.7	17.4	17.3	17.1	17.1	17.1
C-3-*O*	Ara	Glc	Glc	Ara	Ara	Ara	Ara
1′	104.9	104.9	105.1	104.9	104.8	104.8	104.8
2′	74.8	76.9	77.0	74.7	74.6	74.6	74.7
3′	82.5	88.2	88.2	81.7	81.8	81.8	81.7
4′	68.5	69.7	69.8	68.3	68.5	68.5	68.6
5′	65.3	78.0	78.1	64.9	65.2	65.2	65.2
6′		62.6	62.6				
	Rha	Rha	Rha	Rha	Rha	Rha	Rha
1″	102.0	101.8	101.8	102.1	102.1	102.1	102.1
2″	72.5	72.5	72.6	72.6	72.6	72.6	72.6
3″	72.5	72.4	72.5	72.5	72.5	72.5	72.5
4″	73.9	73.9	73.9	74.0	73.9	73.9	73.9
5″	70.1	69.8	69.8	70.1	70.1	70.1	70.1
6″	18.6	18.7	18.7	18.6	18.6	18.6	18.6
	Glc	Xyl	Xyl	Xyl	Xyl	Xyl	Xyl
1‴	105.0	105.0	104.9	105.2	105.3	105.3	105.3
2‴	74.9	74.9	74.9	74.6	74.5	74.5	74.5
3‴	78.3	78.3	78.3	77.8	77.8	77.8	77.8
4‴	71.5	70.6	70.7	70.9	70.9	70.9	70.9
5‴	78.6	67.3	67.3	67.0	67.1	67.1	67.1
6‴	62.6						

21,24-cyclodammar-25-ene-3-O-[α-L-rhamnopyranosyl(1→2)][β-D-xylopyranosyl(1→3)]-α-L-arabinopyranoside (**9**): white amorphous powder; ^{1}H and ^{13}C NMR data, see Tables 2 and 3; HR-ESI-MS *m/z* 897.4805 $[M - H]^-$ (Calcd. for $C_{46}H_{73}O_{17}$, 897.4848).

(20S,21S,23S,24S)-3β,20,21,23,25-pentahydroxy-19-oxo-21,24-cyclodammar-3-O-[α-L-rhamnopyranosyl(1→2)][β-D-xylopyranosyl(1→3)]-α-L-arabinopyranoside (**10**): white amorphous powder; ^{1}H and ^{13}C NMR data, see Tables 2 and 3; HR-ESI-MS *m/z* 915.4943 $[M - H]^-$ (Calcd. for $C_{46}H_{75}O_{18}$, 915.4953).

(20S,21R,23R,24R)-3β,20,21,23,25-pentahydroxy-19-oxo-21,24-cyclodammar-3-O-[α-L-rhamnopyranosyl(1→2)][β-D-xylopyranosyl(1→3)]-α-L-arabinopyranoside (**11**): white amorphous powder; ^{1}H and ^{13}C NMR data, see Tables 2 and 3; HR-ESI-MS *m/z* 915.4924 $[M - H]^-$ (Calcd. for $C_{46}H_{75}O_{18}$, 915.4953).

(20S,21S,24S)-3β,20,21,25-tetrahydroxy-21,24-cyc-

lodammar-3-O-[α-L-rhamnopyranosyl(1→2)][β-D-xylopyranosyl(1→3)]-α-L-glucopyranosyl-25-O-β-D-glucopyranoside (**12**): white amorphous powder; ^{1}H and ^{13}C NMR data, see Table 4; HR-ESI-MS *m/z* 1077.5829 $[M-H]^-$ (Calcd. for $C_{53}H_{89}O_{22}$, 1077.5845).

(20S,21R,23R)-3β,20,21-trihydroxy-21,23-epoxydammar-24-ene-3-O-[α-L-rhamnopyranosyl(1→2)][β-D-xylopyranosyl(1→3)]-β-D-glucopyranosyl-21-O-[β-D-glucopyranosyl (1→6)]-β-D-glucopyranoside (**13**): white amorphous powder; ^{1}H and ^{13}C NMR data, see Table 4; HR-ESI-MS *m/z* 1237.6267 $[M-H]^-$ (Calcd. for $C_{59}H_{97}O_{27}$, 1237.6217).

(20ξ,21ξ,23ξ,24ξ)-3β,21,23-trihydroxy-19-oxo-21,24-cycly-20,25-epoxydrammar-3-O-[α-L-rhamnopyranosyl (1→2)][β-D-xylopyranosyl(1→3)]-α-L-arabinopyranoside (**14**): white amorphous powder; ^{1}H and ^{13}C NMR data, see Table 4; HR-ESI-MS *m/z* 897.4807 $[M-H]^-$ (Calcd. for $C_{46}H_{73}O_{17}$, 897.4848).

(20S)-3β,20,21-trihydroxydammar-19-oxo-24-ene-3-O-β-D-xylopyranosyl-(1→2)-β-D-xylopyranosyl-21-O-β-D-glucopyranoside (**15**): white amorphous powder; ^{1}H and ^{13}C NMR data, see Table 4; HR-ESI-MS *m/z* 899.5041 $[M-H]^-$ (Calcd. for $C_{46}H_{75}O_{17}$, 899.5004).

(20S,23ξ,24ξ)-3β,20,21,23,24-pentahydroxydammaraen-3-O-[α-L-rhamnopyranosyl(1→2)][β-D-xylopyranosyl (1→3)]-α-L-arabinopyranoside (**16**): white amorphous powder; ^{1}H and ^{13}C NMR data, see Table 4; HR-ESI-MS *m/z* 903.5293 $[M-H]^-$ (Calcd. for $C_{46}H_{79}O_{17}$, 903.5317).

Acid hydrolysis of compounds and determination of the absolute configuration of resulting sugar

To elucidate the sugar composition of the newly isolated compounds from *G. longipes*, each compound (1.0 mg) was initially hydrolyzed in 1 mL of 6 mol·L^{-1} trifluoroacetic acid (CF_3COOH) at 90 °C for 2 h. Upon cooling to room temperature, the hydrolysates were extracted with chloroform ($CHCl_3$) three times to remove non-polar components, leaving the aqueous layer, which was then evaporated to dryness. The dried residues, each containing the hydrolyzed sugars, were redissolved in 1 mL of anhydrous pyridine. To each solution, L-cysteine methyl ester hydrochloride (1.0 mg) was added to facilitate the derivatization of the sugars, and the mixtures were incubated at 60 °C for 1 hour. Subsequently, isothiocyanate (5 μL) was added to each solution, and the mixtures were further incubated at 60 °C for another hour to complete the derivatization process. Similarly, standard sugar solutions of L-rhamnose, L-arabinose, D-glucose, and D-xylose (5 mg each) were prepared in 5 mL of anhydrous pyridine, with L-cysteine methyl ester hydrochloride (5.0 mg) added to each. After cooling, isothiocyanate (10 μL) was introduced into each solution, and the reactions were maintained at 60 °C for an hour to yield the respective derivatized standards. The derivatized samples and standards were then analyzed using liquid chromatography-mass spectrometry (LC-MS), utilizing a Waters ACQUITY UPLC-Q-TOF MS system equipped with a Waters HSS T_3 column. The mobile phase consisted of 0.1% formic acid in water (A) and acetonitrile (B), with a gradient of 20% to 30% B over 8 minutes. The flow rate was set at 0.6 mL·min^{-1}, and the column temperature was maintained at 40 °C, operating in negative ionization mode. The LC-MS analysis successfully identified the derivatives of the standard sugars, with L-rhamnose, L-arabinose, D-glucose, and D-xylose being detected at retention times (t_R) of 5.38 (*m/z* 431.1318 $[M-H]^-$), 4.00 (*m/z* 417.1146 $[M-H]^-$), 3.68 (*m/z* 447.1243 $[M-H]^-$), and 4.11 (*m/z* 417.1142 $[M-H]^-$), respectively.

Assay for anti-hypoxic activity

PC12 cells were cultured in RPMI 1640 (Sigma, USA) supplemented with 10% fetal bovine serum (Gibco, Life Technologies, USA) and 100 U·mL^{-1} penicillin (Macgene Biotech Co., Ltd, China) in a humidified incubator containing 5% CO_2 at 37 °C. All tested compounds (> 95%) were dissolved in dimethyl sulfoxide (DMSO) in this study. Salidroside (98.3%) was obtained from our laboratory and its structure was confirmed by spectroscopic analysis.

Cell viability was detected using a Cell Counting Kit 8 (CCK8, Dojindo, Japan) assay. PC12 cells were seeded on a 96-well plate with 8000 cells/well. For cells hypoxia treatment, the cells were placed in a hypoxic incubator with 1%O_2/5%CO_2/92%N_2 at 37 °C. After incubation for 24 h, the cells were pretreated with different doses (3, 10, 30 μmol·L^{-1}) of isolated compounds for 6 h and then treated with hypoxia (1% O_2) for 48 h. The normoxia and hypoxia group was added the same amount of DMSO. Salidroside with a concentration of 30 μmol·L^{-1} was used as a positive control. After treatment, the cells were added to CCK-8 solution with 10 μL/well and were incubated for 3 h. Then, the absorbance was measured at a wavelength of 450 nm using a Microplate Reader (BioTek, USA).

Assays for LDH, SOD and MDA

The release of lactate dehydrogenase (LDH), malondialdehyde (MDA) and superoxide dismutase (SOD) were determined, using assay kits (Nanjing Jiancheng Bioengineering Institute, China) according to the manufacture's protocol.

Cell Apoptosis Assay

For apoptosis detection, PC12 cells subjected to hypoxic conditions and treated with the compounds were analyzed using flow cytometry with annexin V-FITC/PI staining. Post-treatment, cells were washed with phosphate-buffered saline (PBS) and stained with Annexin V-FITC and propidium iodide (PI) using a kit from Bimake, Houston, TX, USA, for 15 minutes in darkness at 37 °C. The stained cells were then analyzed using a flow cytometer from BD Bioscience, USA, to determine the percentages of apoptotic cells.

Conclusions

This study successfully isolated and identified sixteen novel dammarane-type triterpenoid saponins (compounds **1–16**), characterized by structurally diverse side chains at C-17, along with twenty-one known analogues from *G. longipes*. Among these, twenty-seven isolates were evaluated for

their anti-hypoxic activities in PC12 cells, revealing that nine gypenosides significantly protected against hypoxia-induced cellular injury. Further investigations into the underlying mechanisms suggested that these compounds exert their protective effects primarily by inhibiting apoptosis and mitigating oxidative stress, thereby safeguarding cells from hypoxia-induced damages. These findings not only augment the spectrum of known saponins, enhancing our understanding of the chemical diversity within *G. longipes*, but also underscore the potential of these isolates for further scientific exploration

Table 4 ^{1}H NMR and ^{13}C NMR data of compounds 12−16 in pyridine-d_5 (δ in ppm, J in Hz).

Position	12		13		14		15		16	
	δ_H	δ_C	δ_H	δ_C	δ_H	δ_C	δ_H	δ_C	δ_H	δ_C
1	0.80 m, 1.42 m	39.7	0.86 m,1.67 m	40.0	0.62 m, 2.61 m	33.6	2.59 m, 0.67 m	33.4	0.84 m, 1.54 m	39.6
2	1.84 m, 2.27 m	26.9	2.54 m	26.7	1.69 m, 2.07 m	27.6	2.03 m, 1.25 m	27.7	1.87 m, 2.07 m	26.7
3	3.39 dd (4.0, 11.7)	88.9	3.34 dd (4.1, 11.8)	88.9	3.33 dd (4.0, 11.8)	87.1	3.36 dd (3.8, 11.5)	87.5	3.31 dd (4.0, 11.9)	88.3
4		39.7		39.7		40.4		40.4		39.8
5	0.72 m	56.7	0.69 m	56.7	1.15 m	54.9	1.15 m	54.6	0.75 m	56.6
6	1.42 m, 1.49 m	18.5	1.36 m, 1.47 m	18.5	1.91 m	17.7	1.68 m, 1.86 m	17.8	1.39 m	18.5
7	1.23 m, 1.51 m	35.7	1.23 m	35.8	1.33 m, 1.64 m	34.8	1.32 m, 1.59 m	34.6	1.24 m, 1.53 m	35.7
8		40.7		40.7		40.1		40.1		40.8
9	1.25 m	51.2	1.25 m	51.2	1.64 m	53.1	1.67 m	52.8	1.35 m	51.2
10		37.0		37.1		52.8		52.8		37.1
11	1.39 m	21.9	1.64 m	21.9	1.18 m, 1.75 m	22.2	1.63 m	22.3	1.45 m	21.9
12	1.51 m, 1.81 m	25.8	1.66 m	25.8	1.15 m, 2.09 m	25.0	1.90 m	24.6	1.45 m, 2.31 m	28.1
13	1.88 m	44.0	2.30 m	41.6	2.56 m	40.6	2.03 m	41.5	2.18 m	41.9
14		50.3		50.3		49.9		50.2		50.5
15	1.07 m, 1.55 m	31.8	1.15 m, 1.74 m	31.7	1.11 m, 1.65 m	32.0	1.12 m, 1.65 m	31.9	1.11 m, 1.65 m	31.7
16	2.56 d (11.1)	27.7	2.37 m	27.0	2.35 d (12.3)	27.0	1.61 m, 2.04 m	27.7	1.98 m, 2.03 m	24.9
17	2.15 m	47.6	1.98 m, 2.49 m	45.2	1.68 m	44.7	2.22 m	46.0	2.40 m	46.6
18	0.96 s	15.7	0.89 s	15.9	0.87 s	16.0	0.88 s	15.9	0.97 s	15.8
19	0.79 s	16.6	0.75 m	16.6	10.33 s	205.7	10.3 s	205.6	0.79 s	16.6
20		88.3		84.7		91.0		75.5		76.9
21	4.15 m	77.6	5.41 d (7.9)	98.5	5.07 m	78.5	4.05 d (10.2) 4.39 d (10.2)	75.3	4.09 m	67.0
22	1.75 m, 1.96 m	31.6	2.54 m	44.8	1.93 m, 2.16 m	39.6	1.90 m, 2.10 m	36.6	2.24 m, 2.59 m	34.1
23	1.50 m	23.2	5.47 m	73.9	4.72 m	66.2	2.32 m, 2.47 m	23.3	4.62 m	72.8
24	2.81 m	53.3	5.82 m	129.0	2.44 m	57.3	5.46 t (6.6)	126.0	3.87 m	80.1
25		79.9		133.3		78.8		130.8	2.04 m	26.8
26	1.55 s	22.4	1.66 s	25.8	1.81 s	29.7	1.66 s	25.8	1.54 s	25.9
27	1.58 s	27.5	1.64 s	18.1	1.37 s	27,8	1.63 s	17.6	1.50 s	26.2
28	1.26 s	27.9	1.20 s	27.8	1.26 s	26.4	1.25 s	26.5	1.21 s	28.0
29	1.20 s	16.9	1.14 s	16.9	1.10 s	16.1	1.16 s	16.4	1.14 s	16.7
30	0.91 s	16.6	0.98 s	16.8	0.91 s	17.2	0.97 s	17.2	0.98 s	16.8
C-3-*O*	Glc		Glc		Ara		Xyl		Ara	
1′	4.92 d (7.6)	105.0	4.87 d (7.6)	104.9	4.90 d (5.6)	104.9	4.89 d (7.2)	106.2	4.95 d (5.3)	104.8
2′	4.27 m	77.0	4.00 m	77.0	3.94 t (7.6)	74.6	4.20 m	83.5	3.95 t (7.44)	74.7
3′	4.21 m	88.2	4.18 m	88.3	4.29 m	81.9	4.24 m	78.2	4.33 m	81.6
4′	4.04 m	69.8	3.98 m	69,8	4.49 brs	68.6	4.28 m	71.1	4.51 brs	68.3
5′	3.93 m, 4.12 m	78.1	3.92 m	78.0	3.83 d (10.4), 4.30 m	65.2	3.75 m, 4.35 dd (4.5, 11.0)	67.2	3.87 m, 4.36 m	64.9
6′	4.31 m, 4.54 m	62.6	4.34 m, 4.54 m	63.0						
	Rha		Rha		Rha		Xyl		Rha	
1″	6.49 s	101.8	6.48brs	102.1	6.18 s	102.1	5.31 d (7.8)	107.4	6.17 s	102.1
2″	4.63 m	72.6	4.61 m	72.6	4.60 m	72.6	4.18 m	76.3	4.61 m	72.6
3″	4.83 m	72.5	4.75 m	72.5	4.77 m	72.5	4.23 m	69.4	4.76 m	72.5
4″	4.33 m	73.9	4.30 m	74.0	4.29 m	73.9	4.21 m	67.1	4.30 m	74.0
5″	4.80 m	69.9	4.61 m	70.1	4.59 m	70.1	3.75 m, 4.45 dd (4.9,11.0)	71.8	4.62 m	70.1
6″	1.71 d (6.1)	18.7	1.62 d (5.3)	18.6	1.61 d (6.2)	18.6			1.65 d (6.2)	18.6
	Xyl		Xyl		Xyl				Xyl	
1‴	5.03 m	104.9	5.03 m	105.2	5.03 d (8.6)	105.3			5.05 d (7.5)	105.2
2‴	4.00 m	74.9	4.68 t (6.9)	75.2	4.67 t (7.0)	74.6			4.70 t (6.6)	74.6
3‴	4.11 m	78.3	4.13 m	77.8	4.12 m	77.8			4.12 m	77.8
4‴	4.13 m	70.7	4.13 m	70.9	4.13 m	70.9			4.13 m	70.9
5‴	3.72 t (10.5)	67.3	3.68 t (11.1)	67.0	3.68 t (10.6), 4.32 m	67.1			3.68 t (10.7), 4.33 m	67.0

Continued

Position	12		13		14		15		16	
	δ_H	δ_C	δ_H	δ_C	δ_H	δ_C	δ_H	δ_C	δ_H	δ_C
	C-24-*O*-Glc		C-21-*O*-Glc				C-21-*O*-Glc			
1′′′′	5.17 d (7.7)	98.5	6.12 s	104.0			5.05 d (7.6)	106.9		
2′′′′	4.00 m	75.3	4.06 m	75.5			4.08 m	78.6		
3′′′′	4.27 m	78.9	3.97 m	78.5			4.22 m	76.1		
4′′′′	4.16 m	71.9	4.23 m	71.7			4.12 m	71.7		
5′′′′	4.01 m	78.4	4.24 m	77.0			3.98 m	78.6		
6′′′′	4.58 m	63.0	4.36 m, 4.82 m	70.9			4.39 m, 4.57 m	62.8		
			Glc							
1′′′′′			5.05 m	105.9						
2′′′′′			4.13 m	75.2						
3′′′′′			4.22 m	78.4						
4′′′′′			4.18 m	71.9						
5′′′′′			4.25 m	78.3						
6′′′′′			4.32 m, 4.56 m	62.5						

and application in therapeutic contexts.

Supporting Information

The 1D and 2D NMR and HR-ESIMS spectra of compounds **1**–**16** are available as Supporting Information, and can be requested by sending E-mail to the corresponding authors.

References

[1] Wang J, Yang J L, Zhou PP, *et al*. Further new gypenosides from Jiaogulan (*Ggynostemma pentaphyllum*) [J]. *J Agric Food Chem*, 2017, **65**: 5926-5934.

[2] Huang GX, Yasir M, Zheng YL, *et al*. Prebiotic properties of Jiaogulan in the context of gut microbiome [J]. *Food Sci Nutr*, 2022, **1065**: 731-73.

[3] Weng X, Lou YY, Wang YS, *et al*. New dammarane-type glycosides from *Ggynostemma pentaphyllum* and their lipid-lowering activity [J]. *Bioorg Chem*, 2021, **11**: 104843.

[4] Tan HY, Zhang M, Xu L, *et al*. Gypensapogenin H suppresses tumor growth and cell migration in triple-negative breast cancer by regulating PI3K/AKT/NF-κB/ MMP-9 signaling pathway [J]. *Bioorg Chem*, 2022, **126**: 105913.

[5] Zhai XF, Zu ML, Wang YR, *et al*. Protective effects of four new saponins from *Gynostemma pentaphyllum* against hydrogen peroxide-induced neurotoxicity in SH-SY5Y cells [J]. *Bioorg Chem*, 2021, **106**: 104470.

[6] Nguyen NH, Ha TKQ, Yang JL, *et al*. Triterpenoids from the genus *Gynostemma*: chemistry and pharmacological activities [J]. *J Ethnopharmacol*, 2021, **268**: 113574.

[7] Anh PT, Ky PT, Cuc NT, *et al*. Damarane-type saponins from *Gynostemma longipes* and their cytotoxic activity [J]. *Nat Prod Commun*, 2015, **10**: 1351-1352.

[8] Ha TKQ, Pham HTT, Cho HM, *et al*. 12, 23-Dione dammarane triterpenes from *Gynostemma longipes* and their muscle cell proliferation activities *via* activation of the AMPK pathway [J]. *Sci Rep*, 2019, **9**: 1186.

[9] Pham HTT, Ha TKQ, Cho HM, *et al*. Insulin mimetic activity of 3, 4-*seco* and hexanordammarane triterpenoids isolated from *Gynostemma longipes* [J]. *J Nat Prod*, 2018, **81**: 2470-2482.

[10] Schild L, Roth A, Keilhoff G, *et al*. Protection of hippocampal slices against hypoxia/hypoglycemia injury by a *Gynostemma pentaphyllum* extract [J]. *Phytomedicine*, 2019, **16**: 734-743.

[11] Wang J, Zhao M, Cheng X, *et al*. Dammarane-type saponins from *Gynostemma pentaphyllum* prevent hypoxia-induced neural injury through activation of ERk, AKT, and CREB pathways [J]. *J Agric Food Chem*, 2020, **68**: 193-205.

[12] Yin F, Hu LH. Six new triterpene saponins with a 21, 23-lactone skeleton from *Gynostemma pentaphyllum* [J]. *Helv Chim Acta*, 2005, **88**: 1126-1134.

[13] Liu X, Ye WC, Mo ZY, *et al*. Five new ocotillone-type saponins from *Gynostemma pentaphyllum* [J]. *J Nat Prod*, 2004, **67**: 1147-1151.

[14] Huang YP, Wang YS, Liu BW, *et al*. Dammarane-type saponins with proprotein convertase subtilisin/kexin type 9 inhibitory activity from *Gynostemma pentaphyllum* [J]. *Phytochemistry*, 2022, **194**: 113005.

[15] Pang X, Wan LF, Yang J, *et al*. Steroidal saponins from *Trillium tschonoskii* rhizome repress cancer stemness and proliferation of intrahepatic cholangiocarcinoma [J]. *Bioorg Chem*, 2022, **121**: 105679.

[16] Yin F, Zhang YN, Yang ZY, *et al*. Nine new dammarane saponins from *Gynostemma pentaphyllum* [J]. *Chem Biodivers*, 2006, **3**: 771-782.

[17] Yin F, Hu LH, Lou FC, *et al*. Dammarane-type glycosides from *Gynostemma pentaphyllum* [J]. *J Nat Prod*, 2004, **67**: 942-952.

[18] Yin F, Hu LH, Pan RX. Novel dammarane-type glycosides from *Gynostemma pentaphyllum* [J]. *Chem Pharm Bull*, 2004, **52**: 1440-1444.

[19] Gan ML, Liu MT, Gan LS, *et al*. Dammarane glycosides from the root of *Machilus yaoshansis* [J]. *J Nat Prod*, 2012, **75**: 1373-1382.

[20] Shi L, Cao JQ, Li W, *et al*. Three new triterpene saponins from *Gynostemma pentaphyllum* [J]. *Helv Chim Acta*, 2010, **93**: 1785-1794.

[21] Liu J, Li YF, Shi HM, *et al*. Components characterization of total tetraploid jiaogulan (*Gynostemma pentaphyllum*) saponin and its cholesterol-lowering properties [J]. *J Funct Foods*, 2016, **75**: 542-555.

[22] Wang W, Zhao Y, Rayburn E, *et al*. *In vitro* anti-cancer activity and structure-activity relationships of natural products isolated from fruits of *Panax ginseng* [J]. *Cancer Chem Pharm*, 2007, **59**: 589-601.

Cite this article as: LIANG Haizhen, CHEN Xiaojuan, LI Qi, *et al*. Dammarane-type triterpenoids from *Gynostemma longipes* and their protective activities on hypoxia-induced injury in PC12 cells [J]. *Chin J Nat Med*, 2024, **22**(5): 466-480.